

Physical Layer Cognition of FBMC-based Wideband Networking Waveform of SDR



Author

Amna Javed Tiwana

00000204742

Supervisor

Dr. Muhammad Zeeshan

DEPARTMENT OF ELECTRICAL ENGINEERING
COLLEGE OF ELECTRICAL & MECHANICAL ENGINEERING
NATIONAL UNIVERSITY OF SCIENCES & TECHNOLOGY
ISLAMABAD

2020

Physical Layer Cognition of FBMC-based Wideband Networking
Waveform of SDR

Author

Amna Javed Tiwana

00000204742

Thesis submitted in partial fulfillment of the requirements for the degree of

MASTER OF SCIENCE

in

ELECTRICAL ENGINEERING

Thesis Supervisor

Dr. Muhammad Zeeshan

Thesis supervisor's signature:  _____

DEPARTMENT OF ELECTRICAL ENGINEERING
COLLEGE OF ELECTRICAL & MECHANICAL ENGINEERING
NATIONAL UNIVERSITY OF SCIENCES & TECHNOLOGY

ISLAMABAD

2020

Declaration

I certify that this research work titled “**Physical Layer Cognition of FBMC-based Wideband Networking Waveform of SDR**” is my own work. The work has not been presented elsewhere for assessment. The material that has been used from other sources it has been properly acknowledged / referred.



Signature of Student

Amna Javed Tiwana

2020-NUST-MS-ELECT-00000204742

Plagiarism Certificate (Turnitin Report)

This thesis has been checked for Plagiarism. Turnitin report endorsed by Supervisor is attached.



Signature of Student

Amna Javed Tiwana

00000204742



Signature of Supervisor

Copyright Statement

- Copyright in text of this thesis rests with the student author. Copies (by any process) either in full, or of extracts, may be made only in accordance with instructions given by the author and lodged in the Library of NUST College of E&ME. Details may be obtained by the Librarian. This page must form part of any such copies made. Further copies (by any process) may not be made without the permission (in writing) of the author.
- The ownership of any intellectual property rights which may be described in this thesis is vested in NUST College of E&ME, subject to any prior agreement to the contrary, and may not be made available for use by third parties without the written permission of the College of E&ME, which will prescribe the terms and conditions of any such agreement.
- Further information on the conditions under which disclosures and exploitation may take place is available from the Library of NUST College of E&ME, Rawalpindi.

Acknowledgements

Firstly, I would like to pay special regards to my adviser Dr. Muhammad Zeeshan, Assistant Professor at Department of Electrical Engineering, for his assistance, guidance and persistent motivation towards the completion of this research. It has been an honor and true privilege in working with him. Without his constant support and guidance, the goal of this project would not have been realized. I am also obliged to acknowledge my thesis committee members, Prof. Dr. Shahzad Amin Shiekh and Dr. Shahzor Ahmad, from College of E&ME, for being a constant source of encouragement and help throughout my MS course work as well as research work.

I am also indebted to thank my senior Ms. Azka Zaheer, RF Optimization Engineer at Jazz, for providing me with the theoretical concepts of Link Adaptation that has helped me in completing the final phase of my research. I highly value and respect all the instructors and colleagues who have supported and assisted me in various ways all round the execution of this degree.

My profound gratitude goes to my parents and sisters as well, who uplifted my spirits and motivated me to put my best in this period of study from the very beginning till the end.

Abstract

With the fast evolution in wireless communication standards and enhancement in cellular applications, the data rate requirement has increased exponentially over the past few decades. The next generation wireless standards, therefore, need to provide ultra-high data rates with minimum latency. Filterbank Multicarrier (FBMC) system is considered one of most promising techniques so far in order to fulfill such high throughput requirements. Along with that the advent of the era Software Defined Radio (SDR) has made the efficient utilization of Radio Frequency spectrum or resource allocation a crucial parameter to be considered. The need of communication depending upon the available channel conditions, the data rate requirement and the Quality of Service(QoS) according to the application at hand varies vastly. Having significantly reduced side lobes and complete elimination of Cyclic Prefix (CP) as utilized in Orthogonal Frequency Division Multiplexing(OFDM), FBMC provides with minimum Multiple Access Interference (MAI) as compared to the previously used waveform of SDR. Therefore, in order to requisite the high throughput demand, the user requirements and channel quality, an adaptive algorithm should be devised aiding the dynamic selection of optimum parameters providing diverse modes of operation for the type of communication needed. The proposed link adaptation algorithm would incorporate the required data rate, the available channel condition and the Quality of Service demand and would dynamically allocate the optimally selected transmitting end parameters with wideband FBMC waveform for the physical layer of SDR.

Table of Contents

	Page
Declaration	i
Plagiarism Certificate (Turnitin Report)	ii
Copyright Statement	iii
Acknowledgements	iv
Abstract	v
Table of Contents	vi
List of Figures	ix
List of Tables	xi
List of Abbreviations	xiii
 Chapter	
1 Introduction	1
1.1 Objectives and Problem Statement	2
1.2 Thesis Organization	4
2 Literature Review	6
2.1 Software Defined Radio and SDR-waveform	6
2.2 Orthogonal Frequency Division Multiplexing (OFDM) - Preview	8

2.3	QAM to Offset-QAM transformation	10
2.4	FBMC Prototype Filter	12
2.5	Stanford University Interim (SUI) Channel Fading Models	13
2.6	Forward Error Convolutional (FEC) Codes	16
2.7	Link Adaptation	17
3	System Model and Modifications	20
3.1	Analysis of Subcarrier Filters	20
3.2	System Model	21
	3.2.1 FBMC Transceiver Framework	21
	3.2.2 OFDM vs. FBMC Simulation Analysis	23
4	Performance and Parametric Analysis	25
4.1	Performance analysis of FBMC under SUI Channel Models	25
	4.1.1 FBMC/QAM without encoding	25
	4.1.2 FBMC/QAM with encoding	27
	4.1.3 FBMC/OQAM without encoding	28
	4.1.4 FBMC/OQAM with encoding	28
4.2	Parametric Analysis of FBMC/OQAM under SUI Channel Models	30
5	Link Adaptation	33
5.1	Problem Formulation	33

- 5.2 Output MSC (Modulation order, Subcarrier count, Code rate) pairs 36
- 5.3 Data Acquisition for Conditional Rules Formation 37
 - 5.3.1 BER Performance Curves 38
 - 5.3.2 Data Attainment 39
- 5.4 Proposed Condition Algorithm for Link Adaptation 41
 - 5.4.1 Concurring Rules 44
 - 5.4.2 Conflicting Rules 45
 - 5.4.3 Conditional Algorithm Flowchart 49
- 6 Conclusion and Future Work 54
 - 6.1 Conclusion 54
 - 6.2 Future Recommendations 55
- References 56

List of Figures

2.1	SDR - General Block Diagram	8
2.2	OQAM Signal Constellation	11
2.3	Filterbank Illustration	14
3.1	Prototype Filter-bank	21
3.2	OFDM/FBMC Magnitude Response Comparison	22
3.3	FBMC System Model	23
3.4	OFDM vs FBMC Performance Analysis under AWGN Channel	24
3.5	OFDM vs FBMC Performance Analysis under Rician Fading Channel	24
4.1	FBMC/QAM without convolutional encoding	26
4.2	FBMC/QAM with convolutional encoding	27
4.3	FBMC/OQAM without convolutional encoding	28
4.4	FBMC/OQAM with convolutional encoding	29
5.1	BER for various modes of operation in AWGN	38
5.2	BER for various modes of operation in SUI-1	39
5.3	BER for various modes of operation in SUI-4	40
5.4	Conditional Rule based Cognition Engine	42

5.5	Data Acquisition for E_2, S_1, R_1	47
5.6	Data Acquisition for E_3, S_2, R_2	47
5.7	Data Acquisition for E_3, S_1, R_2	48
5.8	Mode selection for QoS of 10^{-2} , SNR from 4dB to 11dB, required data rates range 6Mbps to 8Mbps	48
5.9	Mode selection for QoS of 10^{-3} , SNR from 4dB to 11dB, required data rates range 4Mbps to 6Mbps	52
5.10	Mode selection for QoS of 10^{-3} , SNR from 18dB to 25dB, required data rates range 2Mbps to 4Mbps	52
5.11	Conditional Algorithm Flowchart	53

List of Tables

2.1	f-domain Prototype Filter Coefficients	12
2.2	Terrain Type Classifications	14
2.3	SUI Channel Models Summary	15
2.4	SUI Channel Models - Scenario Specifications	16
4.1	Performance Analytic of FBMC under SUI Channel Models with different cases	30
4.2	Simulation Parameters for Parametric Analysis	30
4.3	Parametric Analysis of FBMC/OQAM under SUI Channel Models with different Parameters	32
5.1	Transmission Parameters for Link Adaptation	35
5.2	Calculated Symbol Duration	35
5.3	Calculated Data Rates for Link Adaptation	36
5.4	Output MSC (Modulation order, Subcarrier count, Code rate) pairs for 18 set of values	37
5.5	Data Acquisition for $M = 2$ in AWGN	41
5.6	Data Acquisition for $M = 4$ in AWGN	42
5.7	Data Acquisition for $M = 2$ in SUI-1	43

5.8	Data Acquisition for $M = 4$ in SUI-1	44
5.9	Data Acquisition for $M = 2$ in SUI-4	45
5.10	Data Acquisition for $M = 4$ in SUI-4	46
5.11	Conditional Rules for AWGN Channel	49
5.12	Conditional Rules for SUI-1 Channel	50
5.13	Conditional Rules for SUI-4 Channel	51

List of Abbreviations

ADC	Analogue to Digital
AFB	Analysis Filter Bank
AMC	Adaptive Modulation and Coding
ASIC	Application-Specific Integrated Circuits
AWGN	Additive White Gaussian Noise
BER	Bit Error Rate
CP	Cyclic Prefix
CQI	Channel Quality Indicator
DAC	Digital to Analogue
DSP	Digital Signal Processor
FBMC	Filterbank Multicarrier
FEC	Forward Error Convolution
FIR	Finite Impulse Response
FIS	Fuzzy Inference System
FPGA	Field Programmable Gate Array
FRBS	Fuzzy Rule Based System
GFDM	Generalized Frequency Division Multiplexing
GPP	General Purpose Processor

HDR Hardware Defined Radio

HPA High Power Amplifiers

HSDPA High-Speed Downlink Packet Access

HSPA High-Speed Packet Access

ICI Inter Channel Interference

ISI Inter Symbol Interference

LOS Line of Sight

LTE Long Term Evolution

MAI Multiple Access Interference

MCDMA Multicode Code Division Multiple Access

MCM Mutlicarrier Modulation

MSC Modulation order, Subcarrier count, Code rate

NLOS Non Line of Sight

OFDM Orthogonal Frequency Division Multiplexing

OQAM Offset Quadrature Amplitude Modulation

PAPR Peak to Average Power Ratio

QoS Quality of Service

RF Radio Frequency

SDR Software Defined Radio

SFB Synthesis Filter Bank

SISO Single-Input Single-Output

SNR Signal to Noise Ratio

SUI Stanford University Interim

TDMA Time Division Multiple Access

UFMC Universal Filter multicarrier

UMTS Universal Mobile Telecommunications System

WiMax Worldwide Interoperability for Microwave Access

Chapter 1

Introduction

The enhancement in the cellular applications and the demand of data usage over the past few decades has risen exponentially. The next generation wireless communication requires ultra-high data rates with minimum latency. Hence the efficient utilization of radio frequency spectrum has become a crucial parameter to be considered for communication. One way to attain this requirement is to use signals with wider bandwidth but wideband signals are subjected to frequency selective fading from the multipath channels. In such cases single carrier systems are not well-suited. To overcome the shortcomings in the single carrier system, Multicarrier Modulation (MCM) was introduced [1–3]. The fading effect is diminished by translating the wideband signal into multiple narrowband signals and each signal is modulated by the subcarriers. Such an arrangement can handle frequency selective fading very effectively.

MCM technique has been utilized in various systems of today, such as WiFi based on the IEEE 802.11 standard, WiMax (Worldwide Interoperability for Microwave Access), based on the IEEE 802.16 standard, OFDM (Orthogonal Frequency Division Multiplexing) based Long Term Evolution (LTE) and LTE-advanced and most recently the potential candidate for 5G, Filterbank Multicarrier (FBMC) modulation [4].

A number of waveform candidates for 5th generation have been introduced over the last two decades including Universal Filter multicarrier (UFMC), Generalized Frequency Division Multiplexing (GFDM), Filtered-OFDM and Filter Bank Multi-Carrier (FBMC) [1,4]. UFMC, Filtered-OFDM and FBMC are derivatives of Orthogonal Frequency Division Multiplexing (OFDM) [5].

Filter Bank Multi-Carrier (FBMC) waveform is one of the most promising 5G candidates so far. Utilizing well-localized filter banks and Offset Quadrature Amplitude Modulation (OQAM) FBMC provides with strict orthogonality as well as eliminates the need of utilizing Cyclic Prefix (CP) in comparison with OFDM [5, 6].

The advent of the era of Software Defined Radios (SDR) rendered possible the software implementation of digital operations without physical human intervention. The multi-mode and multifunctional operation of wireless devices along with the rapid evolution in digital electronics makes the software controlled technology a rather inexpensive, flexible and more viable option [7]. Resource allocation of scarce SDR resources is a dire need of today's modern world, where data rate requirement has been exponentially increasing by every passing day. Another important requirement is variable Quality of Service (QoS) that changes with the application at hand. The channel conditions vary as well from time to time providing with a limited available Signal to Noise Ratio (SNR). All these varying conditions require an adaptable cognition engine that provides the user with an optimum parameter selection of SDR waveform. Such a process is called as Link Adaptation that is a crucial part of SDR waveform design.

In this thesis an enhanced FBMC scheme utilizing OQAM modulation, equalization and convolutional encoding has been implemented. The simulated results are utilized to form output parameter pairs which are then used to form a human intuition based optimum selection scenario. The selection table helps formulating an adaptive algorithm for an effective Link Adaptation process.

1.1 Objectives and Problem Statement

The present-day progress in the in the remote correspondence innovation just as the developing number of remote clients have overburdened the radio recurrence range. Alongside that, a portion of the range groups are tolerably used and some are under used simultaneously. To cater for these spectral wasteful aspects and inefficiencies, some of the current

ideal models like Software Defined Radio and Cognitive Radio have been presented in the course of recent decades [8]. Accordingly an extreme prerequisite of information rate by guaranteeing an ideal Quality of Service (QoS) for given channel conditions has become a need, that should be tended to through wideband systems administration waveform. Due to such requirements, the following objectives need to be followed by the future SDR waveform.

- A communication network highly flexible to accommodate a variety of high data rate applications (QoS)
- Utilizing a wideband scheme that has an ability to cater for most of the effects of multipath fading
- To employ a well-localized system that provides with higher spectral efficiency and finer spectral containment than previously present systems i.e. OFDM
- Capability to provide the user with maximum possible throughput under rigorous channel conditions (SNR)
- Diverse modes of operation according to the given environmental factors such as the required range and available bandwidth/ SNR
- An efficient Link Adaptation algorithm for delivering optimum throughput to the user keeping in view the available channel conditions and user requirements of throughput and QoS

Considering that the present SDR link adaptation algorithms are either MC-CDMA/ adaptive TDMA/ OFDM based with no consideration of user throughput requirement, the aim of this thesis is to develop an adaptive methodology for physical layer cognition of FBMC-based wideband networking waveform of SDR, keeping in view the above mentioned objectives. The research is directed towards the development of a link adaptation algorithm that provides with best possible throughput via a specific set of

FBMC parameters for the required data rate, available Signal to Noise Ratio (SNR) and maximum allowable Bit Error Rate (BER) .

1.2 Thesis Organization

Rest of the thesis is organized as follows.

Chapter 2 provides a detailed literature review of the fundamental concepts and basis for the entire research work, including the basic SDR transceiver and SDR waveform, the fundamental concept of FBMC and how it varies from CP-based OFDM systems, the existing state of the art FBMC system constituents such as the prototype filter and offset QAM modulation, SUI-fading channel models, and an overview of link adaptation and adaptive modulation and coding algorithm for SDR waveform design.

Chapter 3 covers firstly the basic FBMC transceiver model and then incorporates the Rician distribution based SUI channel models in order to introduce real-time based multipath fading environment. The effects of multipath are compensated by the utilization of equalization and convolutional encoding. The AWGN and Rician distribution based fading BER curves for both OFDM and FBMC are compared in this chapter as well.

Chapter 4 presents the simulation results in two parts;

- Part-I provides the BER analysis for 4 different scenarios investigating convolutional encoding and Offset-QAM modulation.
- Part-II depicts the parametric and comparative analysis of FBMC/OQAM model based upon the parameters of modulation order, encoding rate, overlapping factor and number of subcarriers for all 6 SUI channel models.

Chapter 5 presents the proposed novel link adaptation algorithm. AWGN, SUI-1 having light tree density and SUI-4 having moderate-to-heavy tree density channels have

been utilized for final adaptivity algorithms. It involves firstly data acquisition for Fuzzy Rules formation, Output MSC pairs (Modulation order, Subcarrier count, Coding rate) for different set of parameters, a human intuition based MSC pairs selection table based upon user defined inputs i.e. required QoS, Data rate requirement and available SNR and finally coded if-then statements of the obtained pair selection and its incorporation in the final code. The proposed algorithm has been illustrated with the help flowchart.

Finally, chapter 6 concludes the thesis and gives some of the potential future directions in this area of research.

Chapter 2

Literature Review

The demand for incoming wireless technology based applications and newly introduced wireless standards along with the number of users have risen exponentially especially over the past few decades. Keeping in view that the available wireless spectrum is limited and needs to be evenly distributed calls for an efficient resource allocation. In order to support high data rate applications as well as to reconfigure the communication network requirements they are working on, a multicarrier based modulation scheme with an elevated data rate and minimum latency needs to be employed via a re-configurable communication system. The goal of this thesis is to design an adaptive, high throughput FBMC-based link adaptation algorithm for wideband SDR waveform that is flexible enough to allocate its resources on individual basis. In this chapter an architectural review of SDR and SDR waveform, the evolution of CP-based OFDM to FBMC, SUI fading channel models, the existing state of the art FBMC system model and an overview of link adaptation for SDR waveform design has been discussed in detail.

2.1 Software Defined Radio and SDR-waveform

The recent developments and improvements in Field Programmable Gate Array (FPGA), Application-Specific Integrated Circuits (ASICs), Digital Signal Processor (DSP) and General Purpose Processor (GPP), has allowed the researchers to explore the world of re-configurable radios. A traditional radio communication system implemented via hardware components such as modulators/demodulators, mixers, filters and amplifier, etc. is called

as Hardware Defined Radio (HDR). These radios cannot change their configuration according to the user requirement, unless intervened manually. In software defined radios (SDR), once the signal is digitized, the radio functions are implemented using software-driven components [9]. DRs give programming control of an assortment of regulation technique, wide-band or thin band activity, correspondence security capacities (such as frequency hopping), and waveform necessities of current and developing norms over a wide recurrence extend [9, 10]. The SDRs support a broad range of frequency ranges with re-configurable multiple functionality according to the user requirements based on the policies defined in the SDR waveform. According to the FCC a software defined radio can be defined as [11]

”A radio that includes a transmitter in which the operating parameters of frequency range, modulation type or maximum output power (either radiated or conducted), or the circumstances under which the transmitter operates in accordance with Commission rules, can be altered by making a change in software without making any changes to hardware components that affect the radio frequency emissions.”

The term ”Software Radio” was first introduced by a team at the Garland Texas Division of E-Systems Inc.(now Raytheon) in 1984. ”Software Defined Radio” term was first coined by Joseph Mitola in 1992 [12]. Some of the first work on SDRs was undertaken by the Department of Defence (DoD) and ”Joint Tactical Radio Systems”(JTRS) programs in 1997. From architectural point of view most SDRs basically comprise of FPGA, ASICs, DSP and GPP, where the computationally extensive part goes on the FPGA or ASIC and the intelligent part on the DSP or GPP [13]. The general transceiver scheme is shown in the following block diagram Fig. 2.1.

The antenna, Radio Frequency (RF) front-end and Analogue to Digital (ADC)/ Digital to Analogue (DAC) converts of a basic software defined radio are still hardware implemented, whereas the baseband processing such as Timing and Frequency synchronizations, Channel estimation and equalization, Modulation/demodulation, Coding/decoding, Framing, Filtering, MAC/Link layer/Networking protocols, Codec implementation can be achieved by means of software waveform, thus making it a radio whose functionality is

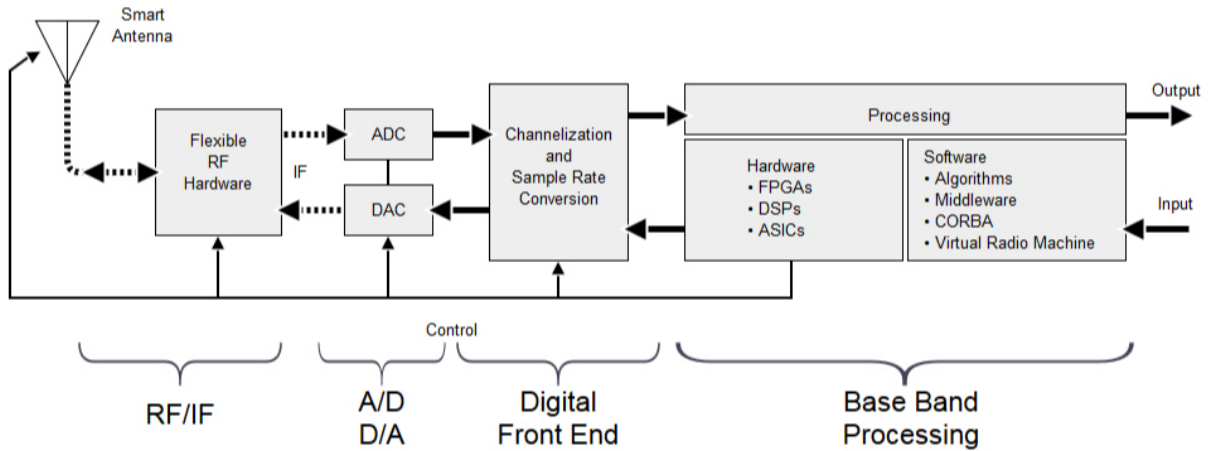


Figure 2.1: SDR - General Block Diagram

controlled by software [14]. A SDR waveform can be characterized as a program through which the Radio Frequency signal, regulation strategy, frequency, conventions, execution and security highlights are characterized and controlled. The waveform is basically defined in terms of specifications such as, frequency range, bandwidth, adaptive throughput capability with multiple modes of operation, maximum required throughput, full duplex voice, video and data communication, IP data communication, multiple levels of security, self healing and self organizing network capabilities, location services, suitable for highly mobile networks etc [10, 15, 16].

2.2 Orthogonal Frequency Division Multiplexing (OFDM) - Preview

One way to attain ultra high data rate requirement is to use signals with wider bandwidth but wideband signals are subject to frequency selective fading from the multipath channels. In such cases single carrier systems are not well suited. To overcome the short comings in single carrier system, Multicarrier Modulation (MCM) is the most prominent technique as it possesses the capability to efficiently cope with frequency selective fading channels and the flexibility to allocate the resources of each subchannel on an individual basis [17]. The

fading effect is diminished by translating the wideband signal into multiple narrowband signals and each signal is modulated by the subcarriers. Such an arrangement can handle frequency selective fading very effectively.

MCM technique has been utilized in various systems of today, such as WiFi based on the IEEE 802.11 standard, WiMax (Worldwide Interoperability for Microwave Access) based on the IEEE 802.16 standard, Orthogonal Frequency Division Multiplexing (OFDM) based Long Term Evolution (LTE) and LTE-advanced and most recently the potential candidate for 5G, Filterbank Multicarrier (FBMC) modulation.

The OFDM system is a well-known MCM approach and one of the most investigated scheme realizing CP-based symbols. Having the frequencies of the subcarriers firmly stuffed and set symmetrical to one another, a high information rate is accomplished and the rest of the ISI is evacuated by augmentation of OFDM image with the Cyclic Prefix (CP). In addition, diminishing the computational prerequisites of the range detecting calculation, effective range usage, adjustment to nature and better in-between operability makes it an alluring innovation for CR-based frameworks [18–20]. The baseband signal in case of CP-OFDM is given as [21],

$$x[i] = \frac{1}{\sqrt{N}} \sum_{n=0}^{N-1} \sum_{m=-\infty}^{\infty} s_{m,n} g[i - mN] e^{j \frac{2\pi}{N} ni} \quad (2.1)$$

where, n denotes the subcarrier index, the data transmitted on the n th subcarrier of the m th OFDM symbol is expressed as $s_{m,n}$ which is a QAM symbol, N represents the total number of subcarriers in one OFDM symbol, the factor $\frac{1}{\sqrt{N}}$ is inserted for power normalization, and h is the rectangular window function that separates the sub-channels, with its time domain coefficients defined as,

$$h[i] = \begin{cases} \frac{1}{\sqrt{T}} & \text{if } |i| \leq \frac{T}{2} \\ 0 & \text{if } |i| > \frac{T}{2} \end{cases} \quad (2.2)$$

where, $T = \frac{1}{\Delta f} = NT_s$ is the OFDM symbol duration, T_s is the sampling interval and f is the subcarrier spacing. For the Inter Symbol Interference (ISI) and Inter Channel Interference (ICI) cancellation, a CP of length L_{cp} is added to the OFDM symbol whose length is equal or greater than the channel delay spread. Although the use of CP ensures the elimination of both ISI and ICI for transmission, however, the Signal to Noise Ratio (SNR) is reduced by a factor $\alpha = \frac{N}{N+L_{cp}}$ [22]. Because of huge frequency domain wavelets, MAI cancellation necessity, higher susceptibility to carrier frequency offset (CFO) and spectral spillage issues, OFDM unquestionably required execution enhancement [23].

2.3 QAM to Offset-QAM transformation

As compared to OFDM, in order to maintain the orthogonality requirement in FBMC each subcarrier is modulated with a real-valued symbol. To keep the same data rate as OFDM system without CP, the FBMC system transmits a real symbol every half symbol duration i.e. $T = 2$, resulting in so called FBMC/OQAM system [24]. At the transmitting end the QAM symbols are transmitted in such a way that the complex modulated symbols are separated into real and imaginary components, the in-phase and quadrature components are then staggered in time by half a symbol period i.e. $T/2$, providing us with OQAM symbols. The complex input symbols are given as,

$$s_n[i] = s_n^I[i] + s_n^Q[i] \quad (2.3)$$

where, $s_n[i]$ is the complex QAM symbol, $s_n^I[i]$ is the real or in-phase part and $s_n^Q[i]$ is the imaginary or quadrature part. These components can be further elaborated as,

$$s_n^I[i] = \sum_{n=0} s_n^I[i] \delta(t - nT) \quad (2.4)$$

$$s_n^Q[i] = \sum_{n=0} s_n^Q[i] \delta(t - nT) \quad (2.5)$$

The basic advantage for utilizing OQAM instead of QAM is that in Quadrature Amplitude Modulation the phase change that could occur at every interval could be very large. When carrier phase shifts by π there is sudden zero-crossing, causing the amplitude to go through zero. So a huge phase change takes place within a short duration of time and as a result huge spectral side lobes are obtained. If we replace QAM with OQAM then only one of these components (In-phase/Quadrature) is changing within an interval T instead of varying simultaneously [24, 25]. When the even component changes the odd one continues to remain in the same phase. This results in a phase shift of only $\frac{\pi}{2}$ instead of π . So there is no sudden zero crossing in the carrier phase. This reduces the spectral growth as compared to when using complex QAM symbols.

The signal constellation can be elaborated via gray-mapping and is shown in the Fig. 2.2.

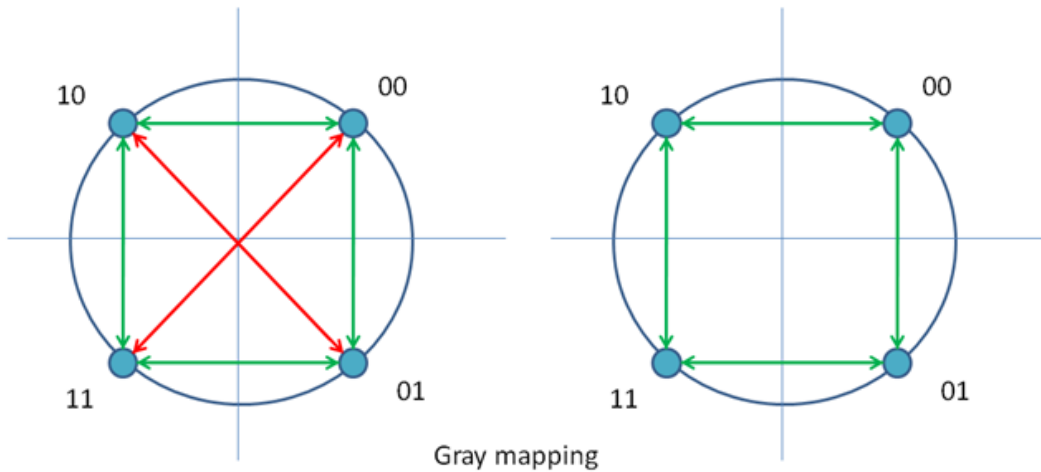


Figure 2.2: OQAM Signal Constellation

2.4 FBMC Prototype Filter

A number of waveform candidates for 5th generation include Universal Filter multicarrier (UFMC) [26], Generalized Frequency Division Multiplexing (GFDM) [27], Filtered-OFDM and Filter Bank Multi-Carrier (FBMC) [6, 28].

Filter Bank Multi-Carrier (FBMC) waveform accompanied with Offset Quadrature Amplitude Modulation (OQAM) is an OFDM based scheme utilizing OQAM for modulating each subcarrier along with a well-localized frequency-sampling based prototype filter [29]. The prototype filter is then shifted for each subcarrier in such a way that the resultant filter bank is only overlapping the adjacent subcarrier only. These well localized prototype filtered subcarriers eliminate the use of Cyclic Prefix (CP) as is the case in CP-based OFDM (CP-OFDM) symbols. The OQAM symbols are filtered through a specifically defined prototype filter for the FBMC based system.

The prototype filter is the key constituent for Synthesis Filter Bank (SFB) and Analysis Filter Bank (AFB) as they are the frequency shifted versions of low pass prototype filter frequency response [6]. The PHYDAS project presents the prototype filter as a Finite Impulse Response (FIR) filter that is causal and real-valued. The prototype filter is characterized by the Overlapping Factor K , which is the ratio of filter impulse response to the multicarrier symbol duration. It could be considered as sample numbers which interest when considered in time domain. The frequency coefficients for $K = 2, 3, 4$ are given in the Table 2.1.

Table 2.1: f-domain Prototype Filter Coefficients

K	H_0	H_1	H_2	H_3
2	1	$\frac{\sqrt{2}}{2}$	-	-
3	1	0.911438	0.411438	-
4	1	0.97195983	$\frac{\sqrt{2}}{2}$	0.23514695

The filter response constitutes $2K - 1$ pulses in the frequency domain, giving us a highly frequency selective filter. The impulse response of the prototype filter is obtained by the IFFT of the above mentioned frequency response pulses [6].

$$h(t) = 1 + 2 \sum_{k=1}^{K-1} (-1)^k H\left(\frac{k}{L}\right) \cos\left(\frac{2\pi km}{L}\right) \quad (2.6)$$

here,

$$m = 1, 2, 3, \dots, L - 1$$

L is the prototype filter length and could be of any choice among $L = KM$, $L = KM + 1$ or $L = KM - 1$, where the total number of subcarriers are given by M .

Once the prototype filter is formulated by the Nyquist criteria the filter banks SFB and AFB are formulated by making shifts of k/M in the baseband prototype filter. A part of such formed filterbank is presented in the Fig. 2.3 [6, 30]. The figure explains how the sub-channels overlap with the neighboring sub-channels only. An even sub-channel does not overlap with another even sub-channel, and likewise an odd sub-channel does not overlap with another odd sub-channel.

2.5 Stanford University Interim (SUI) Channel Fading Models

The multipath fading effects greatly affect the characteristics of a wireless signal as it travels from the transmitter antenna to the receiver antenna. The distance between both the antennas, the single or multiple paths taken by the signal, and the environmental obstacles within the path significantly alter the message signal. The received signal contour can be realized from that of the transmitted signal if we have a model of the medium between the two. This model of the medium is called channel model.

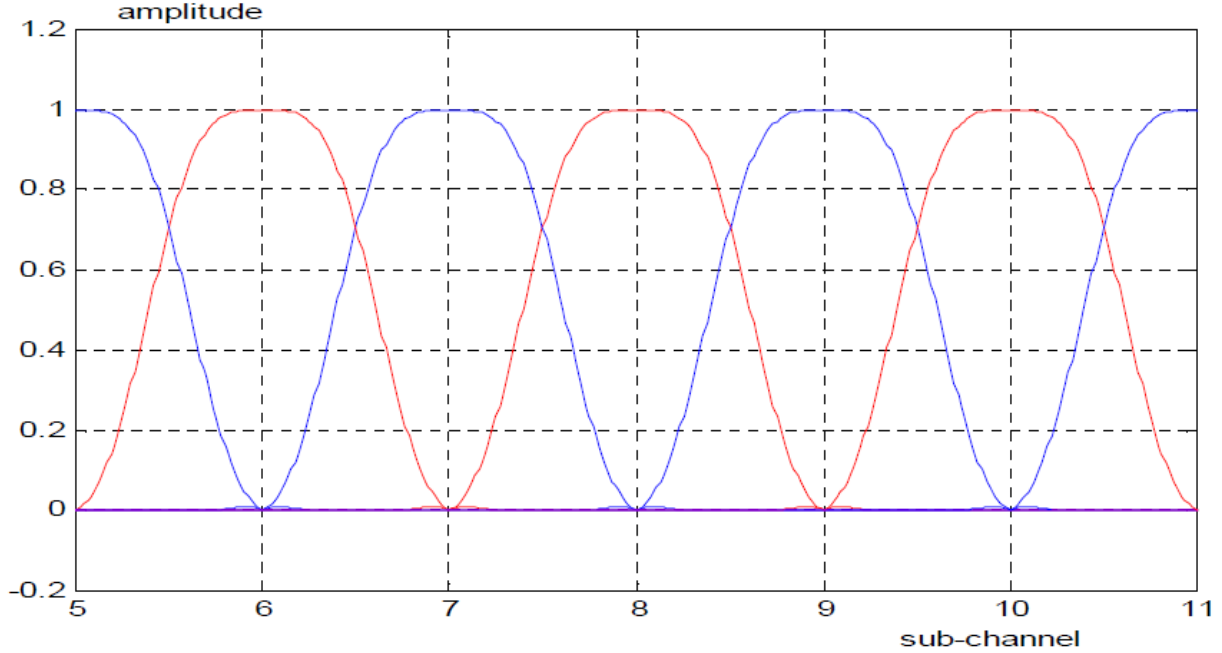


Figure 2.3: Filterbank Illustration

The performance and parametric analysis has been done within a Rician fading environment by incorporating Stanford University Interim (SUI) fading models. The SUI channel models depend on three distinct kinds of landscape (A,B,C), Doppler spreads, delay spread and line-of-sight/non-line-of-site [31,32]. Three classifications of territory types are grouped from a moderate-to-heavy tree thickness with least line-of-sight component, light tree density or medium line-of-sight factor hand a flat terrain type with maximum amount of line-of-sight component, separately presented in the Table 2.2 as well.

Table 2.2: Terrain Type Classifications

A	moderate-to-heavy tree density
B	hilly with light tree density
C	light tree density having a low path loss

The fading is portrayed by the utilization of tapped defer line having 3-taps with non-uniform path delays. The gain associated with each tap is characterized by a Rician

Distribution alongside the maximal Doppler spread. A key factor to be considered is the "K-Factor" or "Rician Factor", that is defined as the ratio of Line of Sight (LOS) component to Non Line of Sight (NLOS) component. If the LOS component is completely eliminated or in other words K-factor is made zero, Rician Distribution turns into Raleigh Distribution.

The mean power specifications are available for both omni-directional as well as 30° antennas. The K-factor values are made available for 90%, 75% and 50% cell coverage areas. The qualities that have been chosen for presenting multipath diversion in this thesis [65] are for an omni-directional antenna with 90% cell inclusion zone; recorded beneath in the Table 2.3.

Table 2.3: SUI Channel Models Summary

SUI Channel No.	Terrain Type	Rician Factor^a (K)	Path Delay Vector (μs)	Path Gain Vector (dB)	Max. Doppler Spread (Hz)
1	C	4	[0 0.4 0.9]	[0 -15 -20]	0.5
2	C	2	[0 0.4 1.1]	[0 -12 -15]	0.25
3	B	1	[0 0.4 0.9]	[0 -5 -10]	0.5
4	B	0	[0 1.5 4]	[0 -4 -8]	0.25
5	A	0	[0 4 10]	[0 -5 -10]	2.5
6	A	0	[0 14 20]	[0 -10 -14]	0.5

^a Omni-directional Antenna

The physical specifications for scenario based SUI channel models are described in a detailed channel modeling analysis in [32] and is tabulated as in Table 2.4.

Table 2.4: SUI Channel Models - Scenario Specifications

Cell Size	7 km
BTS Antenna Height	30 m
Receiver Antenna Height	6 m
BTS Antenna beam Width	120°
Receive Antenna Beam Width	Omni directional (360°) and 30°
Vertical Polarization Only	
90% cell coverage with 99.9% reliability at each location covered	

2.6 Forward Error Convolutional (FEC) Codes

Forward Error Convolutional codes have been researched and utilized in wireless communication networks over the last few decades [33–35]. MCM distribution of the data over multiple carriers renders the subcarriers to cause ISI and ICI over a multipath fading channel, which demands for error correction codes. Channel coding is one such way to rectify the erroneous bits. FEC aims to improve the channel capacity by addition of some redundancy in the form of additional bits along with the information bits. Convolutional codes are typically specified as; (n, k, m) where, n is the number of output bits, k is the number of input bits and m is the number of memory registers or the constraint length [36]. The code rate that defines the amount of redundancy to be added in the input data is given as $R = k/n$. The memory registers or constraint length is obtained as $L = k(m - 1)$, depicting the total number of bits utilized in the encoder memory affecting the generation of output bits.

The concept of convolutional codes was first introduced in 1955 [37] as an alternative to the block codes. Convolutional codes differ from block codes in that the convolutional encoder contains memory and the output at the end of the encoder depends

both on the current input as well as on the m previous inputs. Sequential decoding and threshold decoding were introduced shortly afterwards [38]. Memory is attained by utilizing finite-state shift registers [39–41]. For smaller memory orders Maximum likelihood decoding was proposed in 1967, and termed as Viterbi decoding together with improved sequential decoding techniques [42].

As an alternative way convolutional codes could be represented by different graphical figures such as Tree diagram, Trellis diagram and State diagrams. The Viterbi decoding involves calculating the Hamming distance between the received sequence and each of all the code sequences that arrive at that instant, at a specific trellis state. The procedure is done for all trellis states and time instances for locating minimum Hamming distance path [43, 44]. Such type of decoding is termed as Hard-Decision decoding. Contrary to this, the decoding done on the basis of log-likelihood function is called the Soft-Decision decoding. Furthermore practical considerations reveal that hard-decision decoding reduce the performance gains by approximately 2 dB for Additive White Gaussian Noise (AWGN) channel when compared with the soft-decision decoding [36].

For applications requiring high convolutional rates, high number of branches enter each state and consequently higher number of metric computations per state for Viterbi algorithm. To avoid the computational complexity inherent in the implementation of the decoder of a high-rate convolutional code, **Punctured Convolutional** [45, 46] codes were introduced. The process is done by creating a periodically time varying trellis codes from periodically deleting selected bits from the output of the encoder and thus achieving a higher convolutional code rate from the parent code.

2.7 Link Adaptation

With the recent advancement in wireless communication applications over past few decades and the enhanced number of users, the radio frequency spectrum scarcity needed to be addressed. Along with that varying requirement of quality of service according to the user

need and changing channel conditions demand the development of a cognition engine that provides with the most suitable transmission parameters with such varying scenarios. This process of modification within system parameters or transmission protocols according to the fluctuating channel conditions, the varying user data rate and the quality of service requirements is termed as link adaptation [47, 48].

High-Speed Packet Access (HSPA), a 3.5G or Turbo 3G communication protocol, allowing Universal Mobile Telecommunications System (UMTS) networks with better data rates, is a typical example of utilizing link adaptation algorithm [47, 49]. In High-Speed Downlink Packet Access (HSDPA) the dynamic access of protocols according to the varying radio link conditions is achieved on the basis of modulation types such as QPSK for noisy channels and 16QAM for clearer channels, and Forward Error Correction (FEC) variable rates such as code rate 1 for clearer channels and 1/3 for fading channels [50].

One of the ways to attain link adaptivity is through Adaptive Modulation and Coding (AMC). The bandwidth efficiency is enhanced by selection of optimal parameters in response to the varying fading channel. One of the earliest AMC techniques was proposed in [51, 52] for WiMAX based wireless networks incorporating an OFDMA system for mobile wireless networks. Another research aspect [53, 54] proposes two strategies dependent upon target BER and maximum throughput approach for mobile-WiMax technology using Software Defined Radio. An adaptive modulation system with a finite number of transmission modes was presented in [55] for underwater for underwater acoustic communications based upon orthogonal frequency-division multiplexing (OFDM). The traditional AMC schemes [56–58] mostly realize the periodic feedback of Channel Quality Indicator (CQI) for the down-link transmissions of LTE systems i.e. from the user towards the base station. The limitation of this approach is that it heavily relies upon the assumed channel model. Along with that the CQI feedback delays may result in throughput losses.

A novel OFDM based AMC algorithm that jointly handles the optimized selection of the AMC modes and the on-chip power management of buffering memories is presented in [59]. Thus in contrast to conventional AMC which realizes the wireless channel condi-

tions only, this research considers both the wireless channel conditions and the buffering memory status. Although the proposed AMC algorithm in this paper enhances energy-efficiency at the receiving end, it results in throughput degradation at the transmitting end and needs to be addressed. Another recent dynamic link adaptation algorithm utilizing Fuzzy Inference Inference System (FIS) for hybrid adaptive Time Division Multiple Access (TDMA)/Multicode Code Division Multiple Access (MCDMA) based wideband networking waveform of SDR was proposed in [60]. A constrained optimization problem is formulated and then solved using Fuzzy Rule Based System (FRBS) in order to reduce packet re-transmission overhead in this paper.

One other recently developed Fuzzy Inference System based AMC proposed in [61] provides with improved OFDM system efficiency. The paper utilizes current modulation, SNR, BER and code rate as input parameters and gives an optimized modulation that is fed back towards the OFDM modulator and demodulator. An improved energy efficiency and spectrum utilization in wireless communication systems was proposed in [62] where instead of utilizing rectangular QAM constellation with two-dimensional square portions, hexagonal QAM modulation in combination with non-binary coding was incorporated and its feasibility and efficiency were evaluated using a software-defined radio (SDR) based prototype. Adaptive modulation in another research [63] is considered in order to calculate the cell coverage radius into a cell for different modulation schemes and also to guarantee a target mean BER. A Continuous Phase Modulation (CPM) based algorithm for simultaneous transmission and reception of signals of multiple users is proposed most recently in [64] with a novel hybrid narrowband/wideband networking waveform for a heterogeneous SDR network.

Chapter 3

System Model and Modifications

Filterbank Multicarrier (FBMC) Modulation is considered as the most encouraging competitor for fifth Generation correspondence. The remarkable evolution of FBMC from OFDM originates majorly by a well-localized prototype filter. In this chapter the magnitude response analysis of OFDM and FBMC subcarrier filters, the basic FBMC framework and the simulation results with M-QAM/PSK modulation along with its comparison with OFDM BER curves, the introduction real-time fading channels and the utilization of convolutional encoding along with equalization to counteract the fading effects have been discussed.

3.1 Analysis of Subcarrier Filters

As stated earlier, FBMC differs from OFDM in that it includes some additional processing in the form a prototype filter based filter bank that eliminates the need of Cyclic Prefix and thus contributes towards better spectral efficiency. The OFDM scheme involves rectangular filtering for symbols in time domain that translates as *sinc* in frequency domain. The FBMC system on the other hand utilizes frequency pulses according to the Table 2.1, that translates to as in equation 2.6 in t-domain.

The spectral analysis is a necessary condition to be observed in order to observe the subcarrier interference between successive symbols. When analyzed in frequency domain for magnitude response analysis the rectangular filter based OFDM give huge side lobes due to *sinc*, thus imposing the orthogonality constraint among all the subcarriers in order to fulfill the Nyquist Criteria i.e. the impulse response of the transmission filter must cross the

zero axis at all the integer multiples of the symbol period [6]. In contrast to this the FBMC system considers the frequency coefficients and then imposes the symmetry condition in order to fulfill Nyquist Criteria. This analogy when shifted for each subcarrier results in the form of a 'filter-bank', having a negligible amplitude beyond the central frequency of the adjacent subcarriers. The filter-bank for an Overlapping factor $K = 4$ as shown in the Fig. 3.1.

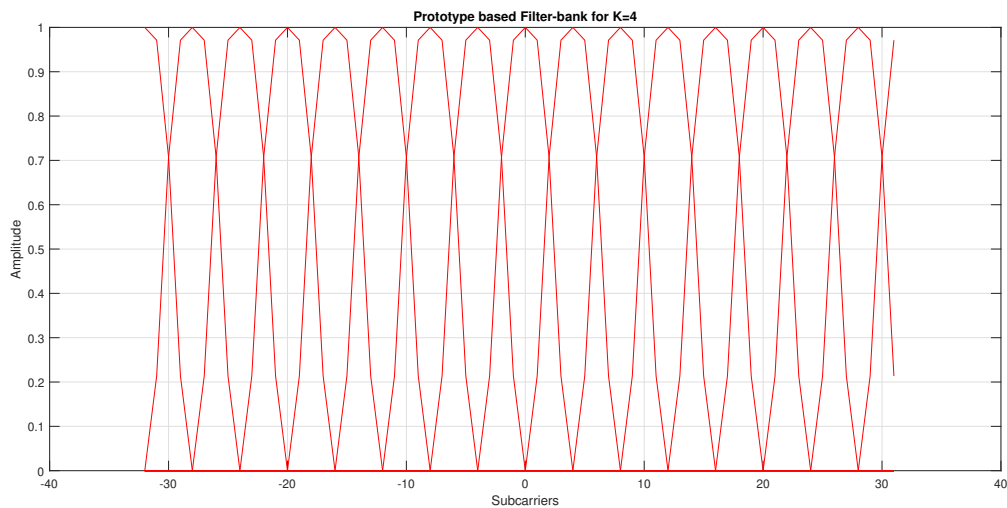


Figure 3.1: Prototype Filter-bank

To summarize FBMC eliminates the need of orthogonality among all the subcarriers unlike OFDM, as any subcarrier overlaps with its immediate neighbors only [6, 23]. Magnitude Response with $M = 256$ subcarriers and an overlapping factor of $K = 4$ is shown in the Fig. 3.2.

3.2 System Model

3.2.1 FBMC Transceiver Framework

After the formulation of Prototype Filter the next step is Poly-phase Filter-banks (SFB and AFB) formulation with frequency shifting in the prototype filter. The elaborated FBMC

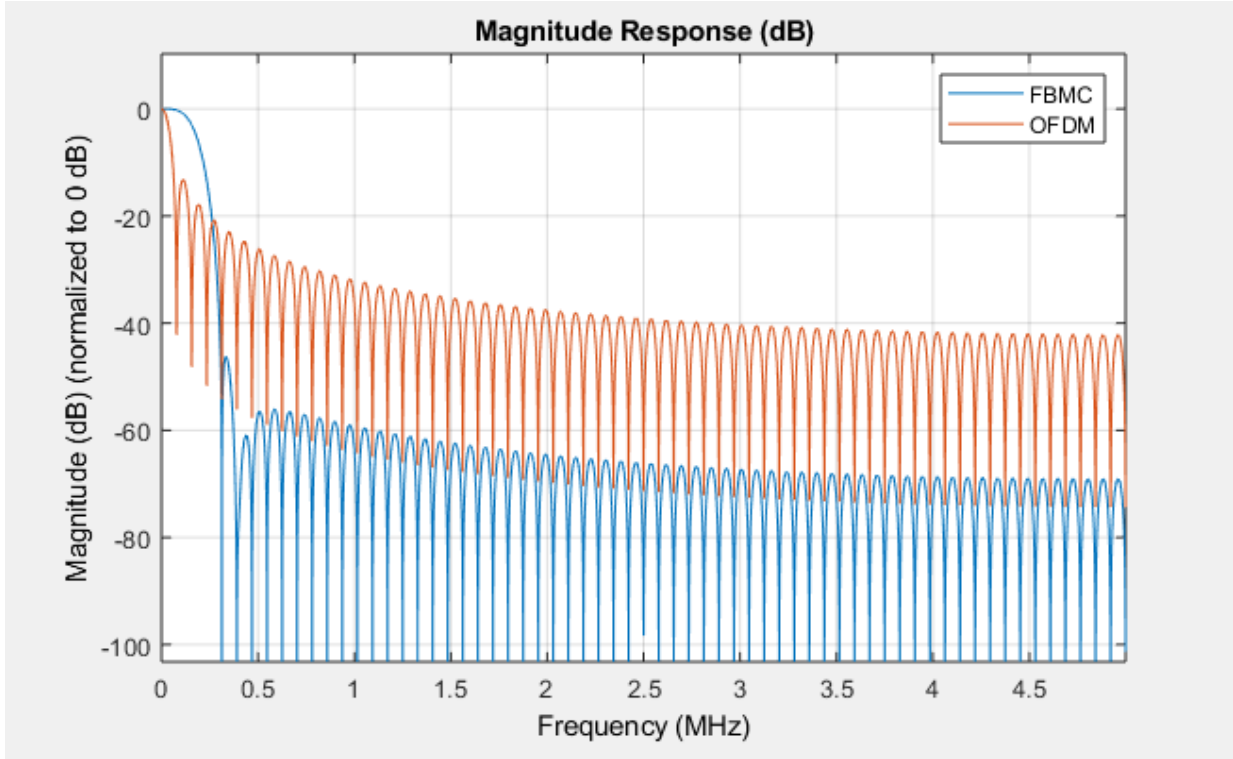


Figure 3.2: OFDM/FBMC Magnitude Response Comparison

transmitter-receiver block diagram with channel encoding, OQAM modulation, filter banks and equalization is shown in the Fig. 3.3. The first step is the addition of redundancy in the source data in the form of convolutional encoding. The code rates that are utilized in our work are 1, 1/2, 2/3. The data is then modulated with QAM/QPSK modulation and then the serial to parallel conversion is made. OQAM modulation as described in the section 2.3 is then implemented in order to gain better spectral efficiency. Finally the modulated data symbols are passed through IFFT based SFB and sent over the multipath fading channel.

At the receiving end, the reverse ordered transmitter blocks are arranged in such a way that noisy data from the frequency selective fading channel is first passed through the FFT based AFB and then equalized in order to cater for the effects of the channel. Although if only AWGN is considered the equalization could be left as there are no mutipath fading effects under consideration.

Once the received data has been equalized, it is passed through OQAM post

processing; where the data that was split into real and complex parts is recombined again and converted back to serial data from the incoming parallel streams. The demodulation is done and then the Viterbi decoding in order to remove the additionally added redundancy via convolutional encoding at the transmitting end. The overall FBMC transceiver is shown in the Fig. 3.3.

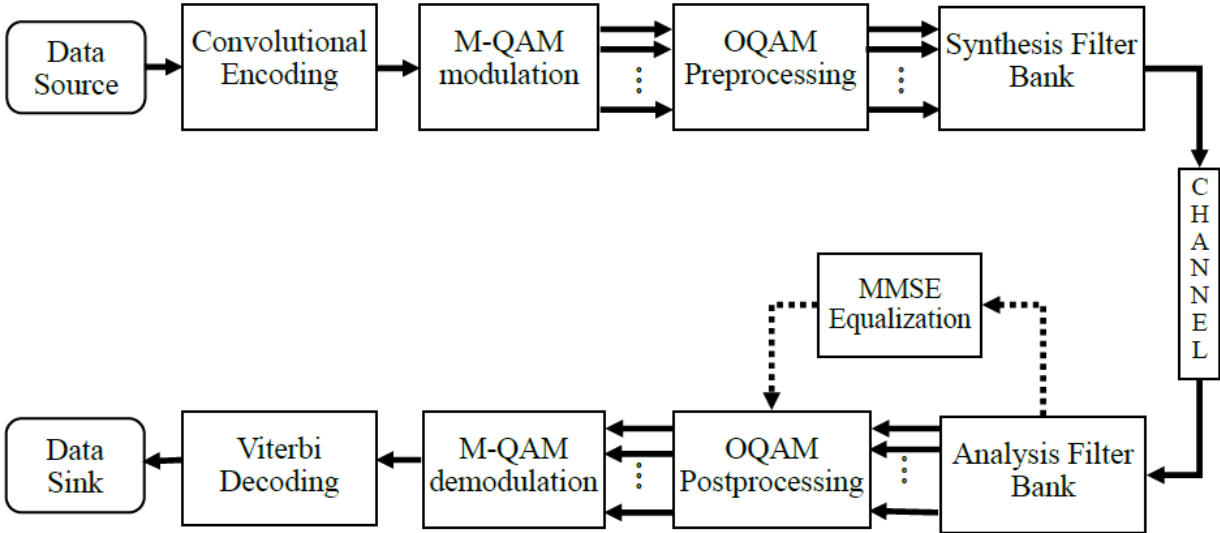


Figure 3.3: FBMC System Model

3.2.2 OFDM vs. FBMC Simulation Analysis

The first performance comparison analysis has been done within AWGN channel environment considering a Single-Input Single-Output (SISO) system and is scrutinized using MATLAB based simulations. The BER vs E_b/N_0 analysis reveals the how well FBMC outperforms OFDM. Normalized Signal to Noise Ratio (SNR) i.e. Energy per bit to Noise power spectral density ratio i.e. E_b/N_0 , is utilized as the bit-transmission is considered. The curves are obtained keeping the subcarrier count $M = 256$, a CP length of $M/4$ for OFDM and an overlapping factor of $K = 4$ in case of both FBMC/QAM and FBMC/OQAM. The AWGN curves are shown in the Fig. 3.4.

The second performance comparison analysis has been done within a multipath

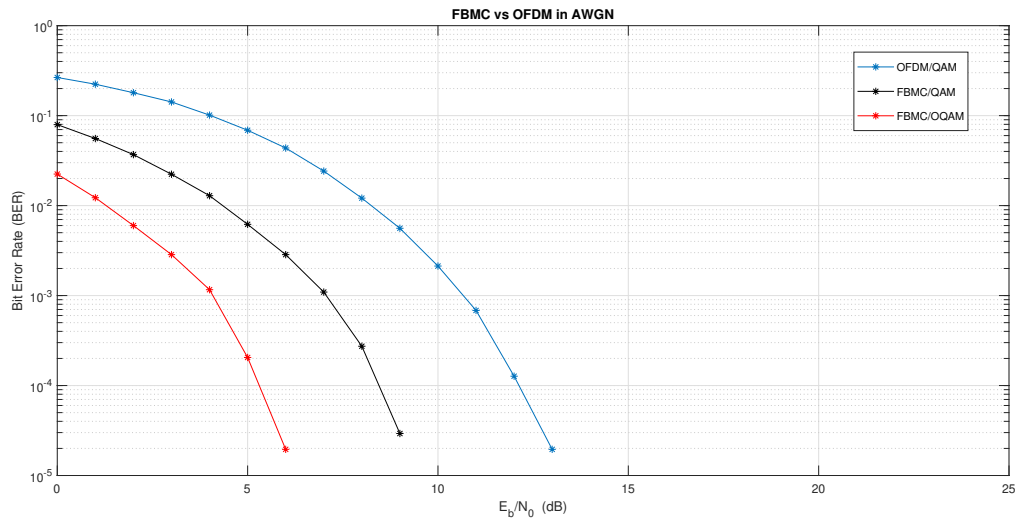


Figure 3.4: OFDM vs FBMC Performance Analysis under AWGN Channel

fading environment by realizing SUI fading channels. The SUI-4 fading channel has been utilized in this research, having a moderate to heavy tree density. The simulation results for FBMC/OQAM are obtained keeping the convolutional encoding rate 1/2 with MMSE equalization. The curves clearly indicate OFDM reaches noise floor on increasing the SNR whereas FBMC significantly outperforms in Rician fading environment as shown in the Fig. 3.5.

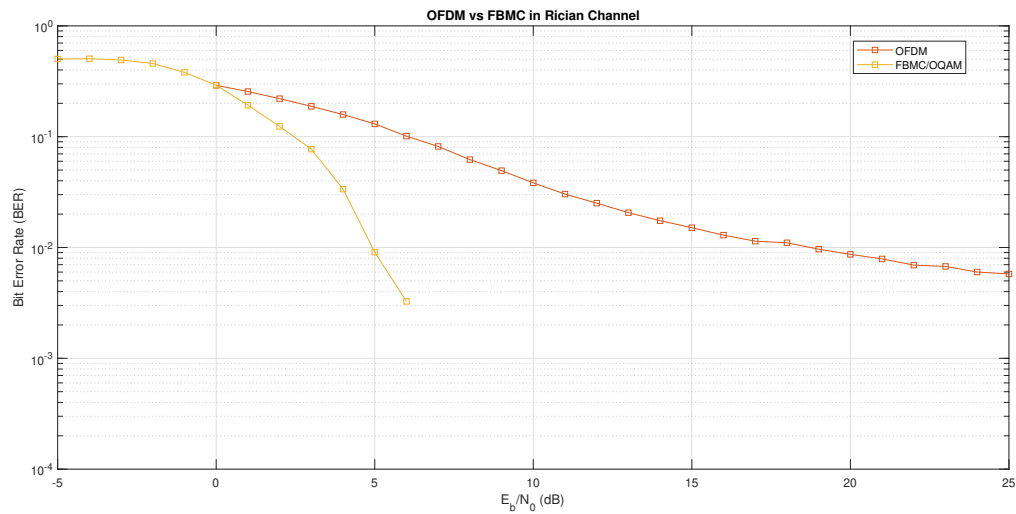


Figure 3.5: OFDM vs FBMC Performance Analysis under Rician Fading Channel

Chapter 4

Performance and Parametric Analysis

The performance and parametric analysis has been performed by for all 6 SUI fading channel models as well as AWGN channel [65]. The simulation results in the form of BER curves along with summarized tabulated results are illustrated in this chapter.

4.1 Performance analysis of FBMC under SUI Channel Models

The performance investigations is performed by observing the effects of convolutional encoding and OQAM modulation under Rician channel environment. The analysis is done under four different scenarios which are mentioned as below.

- FBMC/QAM without encoding
- FBMC/QAM with encoding
- FBMC/OQAM without encoding
- FBMC/OQAM with encoding

4.1.1 FBMC/QAM without encoding

The first case is done with the basic FBMC framework with Single Input Single Output (SISO) model based upon Quadrature Amplitude modulation for 256 subcarriers and an

overlapping factor $K = 4$. The SNR per bit i.e. $\frac{E_b}{N_0}$ is set for the range of $-5 : 25dB$, giving us an SNR range as,

$$SNR_{db} = \frac{E_b}{N_0} + 10\log_{10}(b * rate) \quad (4.1)$$

where, b is bits per subcarrier and $rate$ is the convolutional encoding rate. For performance analysis the modulation order is set as 4 and an encoding rate is set at $1/2$. The simulation curves for AWGN and SUI channels are shown in the Fig. 4.1.

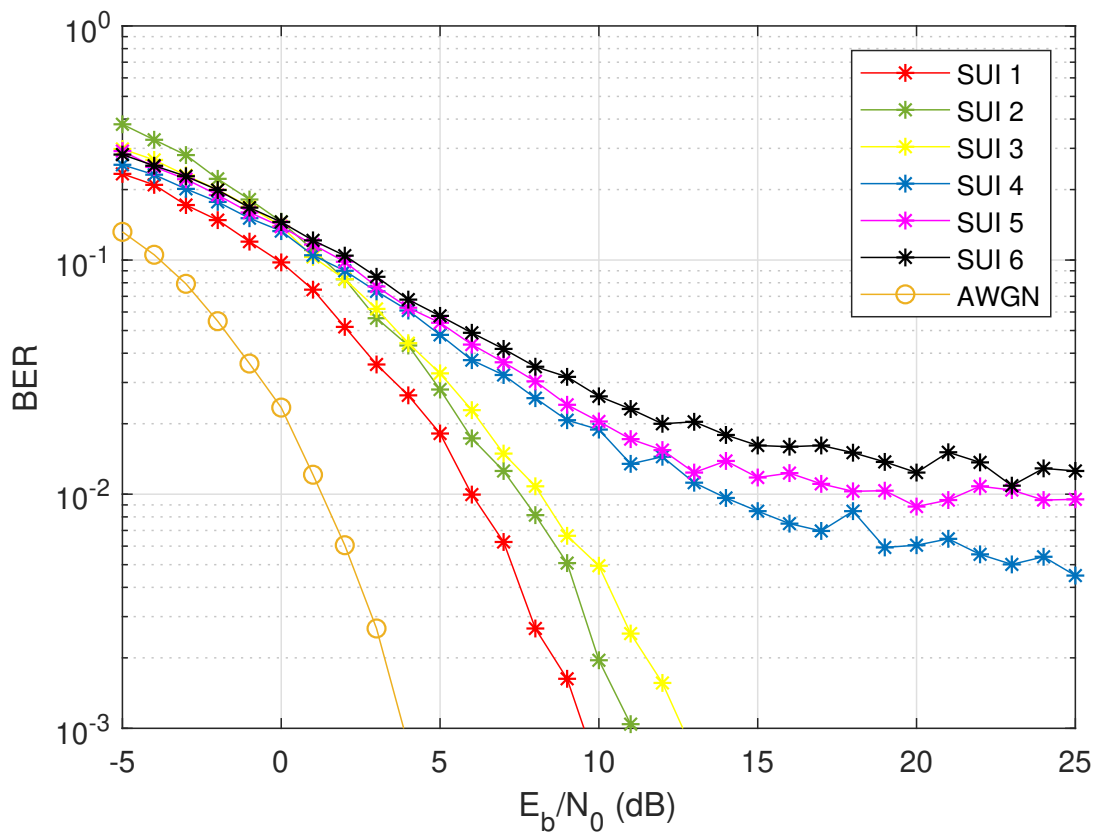


Figure 4.1: FDMC/QAM without convolutional encoding

4.1.2 FBMC/QAM with encoding

In order to gain exemption towards fading path noise, convolutional encoder is utilized in order to add additional bits to the original data according to some specific rule, as described in chapter 2, section 2.6. The encoder allows the convolution of the impulse response of the given input and the encoder. The utilized correction rule in this part is 1/2 so in other words two bits are being provided to the encoder for each bit. Performance curves for this scenario for AWGN as well as SUI channels are shown in the Fig. 4.2. The constraint length for the Convolutional Encoder is kept at 7. Soft decoding for Viterbi decoder is chosen over hard decoding, so as to provide with more precise results.

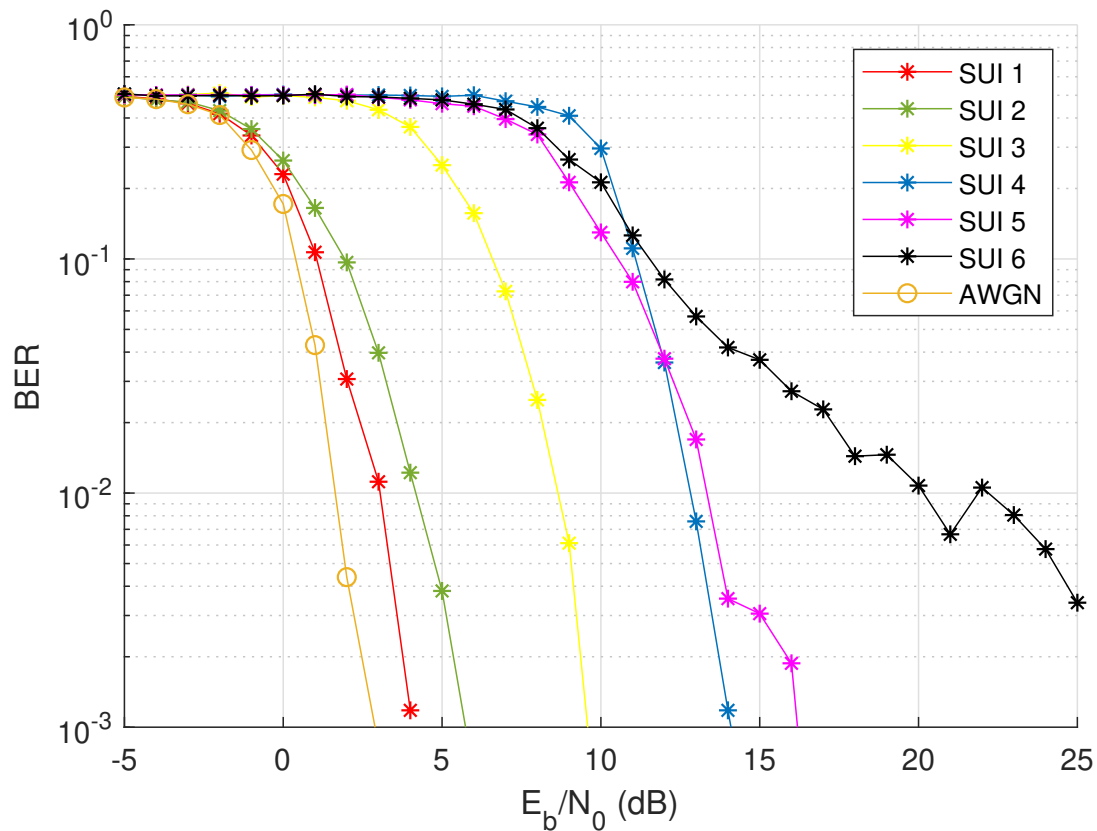


Figure 4.2: FBMC/QAM with convolutional encoding

4.1.3 FBMC/OQAM without encoding

As stated earlier in the chapter 2, section 2.3, the incorporation of OQAM instead of QAM promotes well the overlapping of FBMC symbol with just the adjacent symbol. Unlike QAM, OQAM guarantees that the in-phase and quadrature components of the message symbol are not sent simultaneously. The performance statistics for this scenario are presented in the Fig. 4.3.

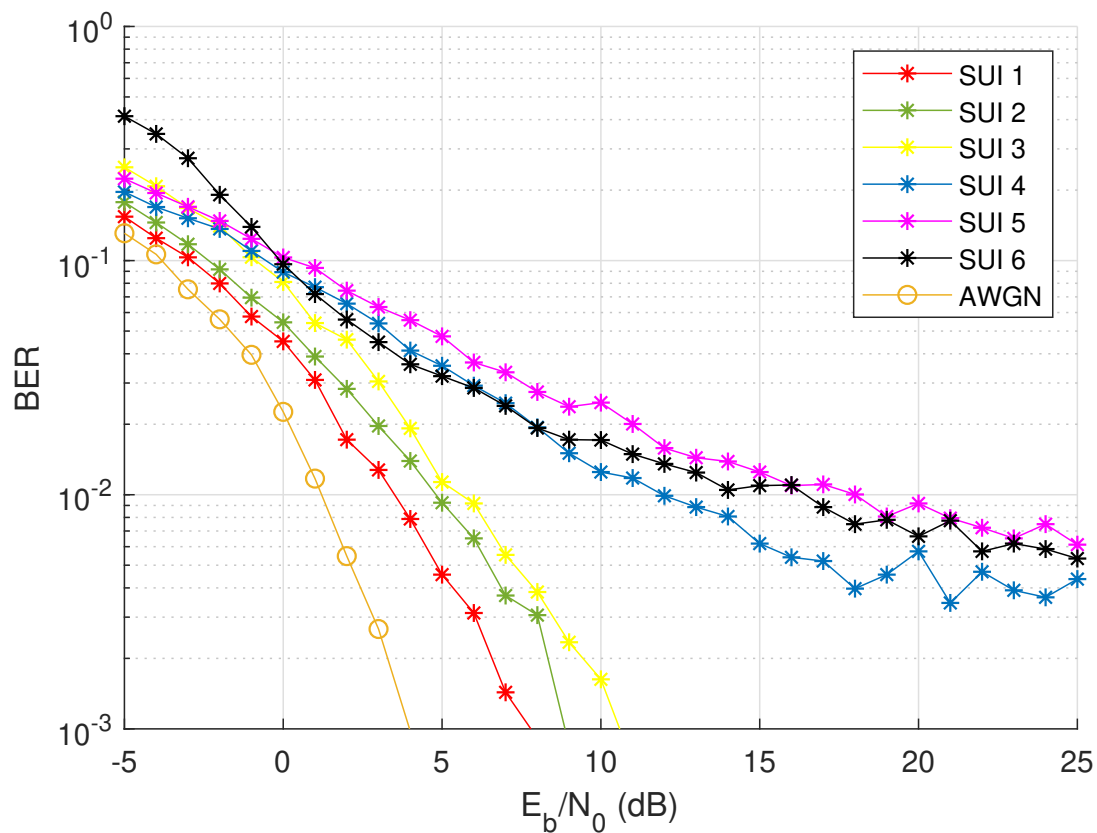


Figure 4.3: FBMC/OQAM without convolutional encoding

4.1.4 FBMC/OQAM with encoding

In the last case the both the adjustments i.e. convolutional encoding along with Offset-QAM modulation, are combined in case 4, in order to obtain maximum orthogonality and

spectral efficiency. The rudimentary system model is kept uniform for each simulation. The curves in final scenario are depicted in the Fig. 4.4.

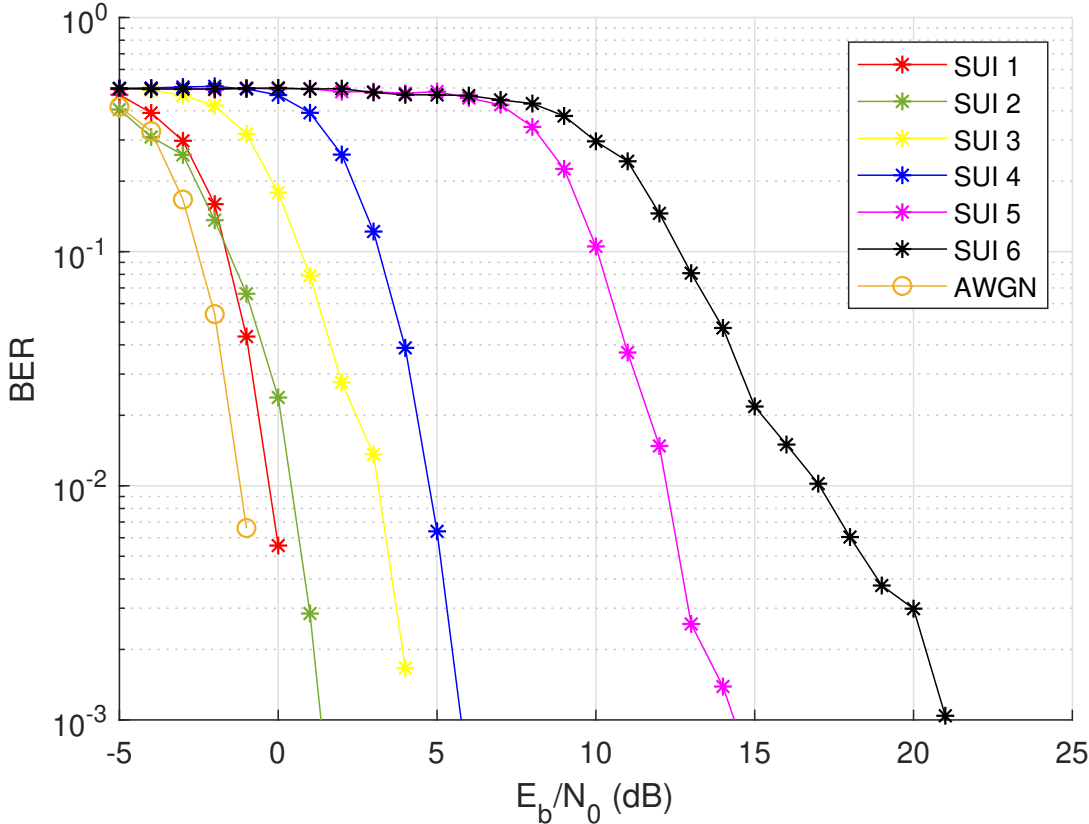


Figure 4.4: FBMC/OQAM with convolutional encoding

The comprehensive performance evaluation is summed up in the Table 4.1 for each case under rician fading environment. The table depicts the findings, at a threshold value at the brink of 10^{-2} . The results clearly indicate the improved BER curves for the last case and worst for first. The results decline significantly when advancing towards SUI-6 channel from SUI-1 channel, as the channel is transcending from light tree density having lesser multipath fading effects towards heavy tree density involving larger interference.

Table 4.1: Performance Analytic of FBMC under SUI Channel Models with different cases

Case No.	AWGN	SUI-1	SUI-2	SUI-3	SUI-4	SUI-5	SUI-6
1	1.319	5.793	7.481	8.52	13.72	18.07	23.07
2	1.642	3.041	4.165	8.152	12.8	13.34	20.15
3	1.191	3.506	5.008	5.863	12.04	16.02	15.03
4	-1.207	-0.2768	0.4017	3.16	4.752	12.22	17.06

4.2 Parametric Analysis of FBMC/OQAM under SUI Channel Models

For parametric analysis under different parameters the SUI-4 channel model is considered, where it is submitted to a variety of order of modulation, prototype filter-overlap value, subcarrier count and convolutional code rates. The employed factors for parametric analysis are sencapsulated in the Table 4.2.

Table 4.2: Simulation Parameters for Parametric Analysis

Parameters	Values
Order of Modulation	2OQAM, 4OQAM
Subcarrier Count	128, 256, 512
Filter-Overlap Values	2, 3, 4
Convolutional Code Rate	1/2, 2/3

The simulation outcomes got by modifying the above mentioned parameters have

been elaborated in the Table 4.3. The Signal to Noise Ratio per bit E_b/N_0 values thus obtained demonstrate the different patterns that the model will in general follow. The addition in filter-overlapping value and subcarrier count refine BER performance. Despite the fact that the decoder proficiency enhances with the constrained length, be that as it may, enhanced constraint length out-tuns in efficient encoding [36]. The limitation (constraint length) is selected to be 7 for a code rate of 1/2 and afterward shifted for a code rate of 2/3. Since the convolutional encoding rate is lower in the previous case, it has better performance curve too.

Table 4.3: Parametric Analysis of FBMC/OQAM under SUI Channel Models with different Parameters

Parameters	AWGN	SUI-1	SUI-2	SUI-3	SUI-4	SUI-5	SUI-6	
Modulation Order	2	-1.401	-0.738	1.448	2.102	6.528	10.46	13.63
	4	-1.217	-0.2768	2.327	4.305	7.201	12.22	16.17
Number of Subcarriers	128	-1.028	1.868	4.463	6.381	8.143	10.42	19.62
	256	-1.217	-0.2768	2.327	4.305	7.201	9.962	16.17
	512	-1.341	-0.8858	1.766	2.601	5.697	8.922	10.06
	2	-1.045	1.955	6.281	7.559	11.32	15.48	22.84
Overlapping Factor	3	-1.089	1.137	3.259	6.238	10.23	13.81	18.36
	4	-1.217	-0.2768	2.327	4.305	7.201	12.22	16.17
Encoding Rate	1/2	-1.217	-0.2768	2.327	4.305	7.201	12.22	16.17
	2/3	-0.4791	0.6101	3.823	7.196	8.512	14.95	19.48

Chapter 5

Link Adaptation

The diverse quality of service requirements varying from voice, text, IP data communication towards HD videos and live streaming, demand efficient resource allocation for SDR-based networks. Along with that high data rates requirement necessitates wideband waveform capable of high speed communication. In addition to that, the time-varying channel conditions and terrain alterations entail a cognitive process for adaptation of transmission parameters, providing optimal service. Such a process is termed as Link Adaptation.

In this chapter the proposed adaptive algorithm for link adaptation based using conditional rule based algorithm for the physical layer of the wideband networking waveform of SDR is discussed in detail. The proposed algorithm is able to provide with most suitable parametric pair values according to the available SNR or required data rate and QoS. The proposed algorithm is done within AWGN channel model, SUI fading channel number 1 having light tree density and a stronger LOS component and SUI fading channel number 4 which models a terrain having moderate-to-heavy tree density and weak to no LOS component in this research.

5.1 Problem Formulation

The optimization problem is based upon the available channel conditions as well as the user requirements. In order to formulate the overall throughput the involved parameters are modulation order, number of subcarriers, symbol time, encoding rate and the available RF bandwidth. The RF bandwidth is considered to be at 5MHz and the throughput

calculation for kth user is given as,

$$R_k = \frac{\log_2(M_k)Nr}{T_{sym}} \quad (5.1)$$

where,

R_k = Throughput for kth user in Mbps

M_k = Modulation order for kth user

$\log_2(M_k)$ = Bits per OQAM symbol for the kth user

N = Total number subcarriers

r = Convolutional rate incorporated for transmission

T_{sym} = Symbol duration

T_{sym} is given by incorporating the RF bandwidth as,

$$T_{sym} = \frac{N}{B_{RF}} \quad (5.2)$$

Utilizing the symbol time in equation 5.1 gives us the final overall throughput for the kth user as,

$$R_k = \log_2(M_k)rB_{RF} \quad (5.3)$$

subjected to the constraints,

$$\text{BER} \leq \text{BER}_{max}$$

$$R_k = \begin{cases} R_{max} & \text{if } R_{max} \leq R_{req} \\ R_{req} & \text{if } R_{max} > R_{req} \end{cases} \quad (5.4)$$

here,

BER = Bit Error Rate

BER_{max} = Maximum allowed BER as per QoS requirement

R_{k,req} = Throughput requirement of kth user/application in Mbps

R_{max} = Maximum throughput possible for given QoS range and SNR

The selected transmission parameters for link adaptation are given in the Table 5.1 and the symbol time based on the number of subcarriers and RF bandwidth are given in the Table 5.2. The symbol duration rises as the number of subcarriers are increased.

Table 5.1: Transmission Parameters for Link Adaptation

Parameters	Values
Modulation Order	2OQAM, 4OQAM
Number of Subcarrier	128, 256, 512
Encoding Rate	1, 1/2, 2/3

Table 5.2: Calculated Symbol Duration

Subcarrier Count	Symbol Time (sec)
128	$2.56e^{-5}$
256	$5.12e^{-5}$
256	$1.024e^{-4}$

The BER range is assumed to be as $10^{-4} \leq \text{BER}_{max} \leq 10^{-1}$ and the calculated data rates in Mbps on the basis of order of modulation, convolutional encoding rate and RF bandwidth are provided in the Table 5.3. The data rates vary within a range of $2.5\text{Mbps} \leq R_{k,req} \leq 10\text{Mbps}$. It should be noted that the rise in number of subcarriers does not affect the throughput but enhances the symbol period. The increase in modulation order or encoding rate on the other hand enhance the throughput without affecting the symbol period.

Table 5.3: Calculated Data Rates for Link Adaptation

Modulation Order	Encoding rate	$R_k(\text{Mbps})$
2	1	5
	1/2	2.5
	2/3	3.33
4	1	10
	1/2	5
	2/3	6.67

5.2 Output MSC (Modulation order, Subcarrier count, Code rate) pairs

For the development of Conditional Rule based algorithm the first step is assignment of MSC (Modulation order, Subcarrier count, Code rate) pairs for 18 pairs/ set of values. The parametric values for order of modulation, number of subcarrier and convolutional encoding rates are listed in the Table 5.3. The MSC pairs are given tabulated in the Table

5.4. Also the utilized notations are as follows,

$\{E_1, E_2, E_3, P_4\}$ = QoS for BER values 10^{-1} to 10^{-4} respectively

$\{S_1, S_2, S_3, S_4\}$ = SNR ranges in either of the above mentioned cases i.e. AWGN, SUI-1/4

$\{R_1, R_2, R_3, R_4\} = R_{k,req}$ according to the user requirement

$\{P_1, P_2, \dots, P_{18}\}$ = MSC output pair for the available SNR, required QoS and Data rate

Table 5.4: Output MSC (Modulation order, Subcarrier count, Code rate) pairs for 18 set of values

Value	MSC	Value	MSC
	Pair		Pair
P_1	(2,128,1)	P_{10}	(4,128,1)
P_2	(2,256,1)	P_{11}	(4,256,1)
P_3	(2,512,1)	P_{12}	(4,512,1)
P_4	(2,128,2/3)	P_{13}	(4,128,2/3)
P_5	(2,256,2/3)	P_{14}	(4,256,2/3)
P_6	(2,512,2/3)	P_{15}	(4,512,2/3)
P_7	(2,128,1/2)	P_{16}	(4,128,1/2)
P_8	(2,256,1/2)	P_{17}	(4,256,1/2)
P_9	(2,512,1/2)	P_{18}	(4,512,1/2)

5.3 Data Acquisition for Conditional Rules Formation

The next step is the data acquisition from BER performance curves for all modes of operation based upon modulation order, encoding rate and number of subcarrier, mentioned in the Table 5.4. The BER curves have been analyzed for the cases of AWGN, SUI-1 and SUI-4.

5.3.1 BER Performance Curves

The BER curves for AWGN, SUI-1 and SUI-4 are obtained for all the parametric pairs in order to obtain data in the next step. As an example three performance curves for P_1 , P_6 and P_{13} are shown in the Fig. 5.1, Fig. 5.2 and Fig. 5.3, respectively.

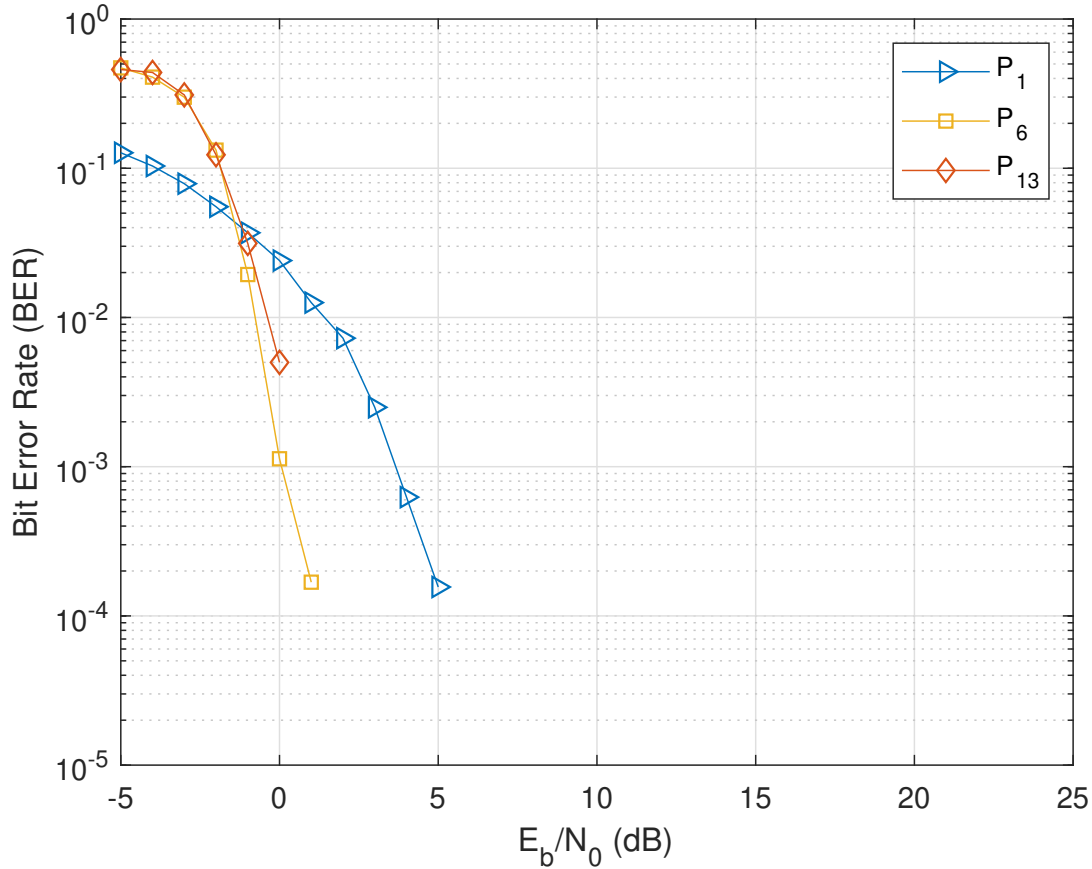


Figure 5.1: BER for various modes of operation in AWGN

The performance for P_1 is the worst as the convolutional encoding for this mode is 1 i.e. uncoded whereas the best case here is obtained when the number of subcarriers is increased to 512 i.e. mode P_6 . As there are no multipath fading effects in the case of AWGN, the increase in subcarrier count has a minute effect on performance. The variations are more apparent in the SUI-4 case.

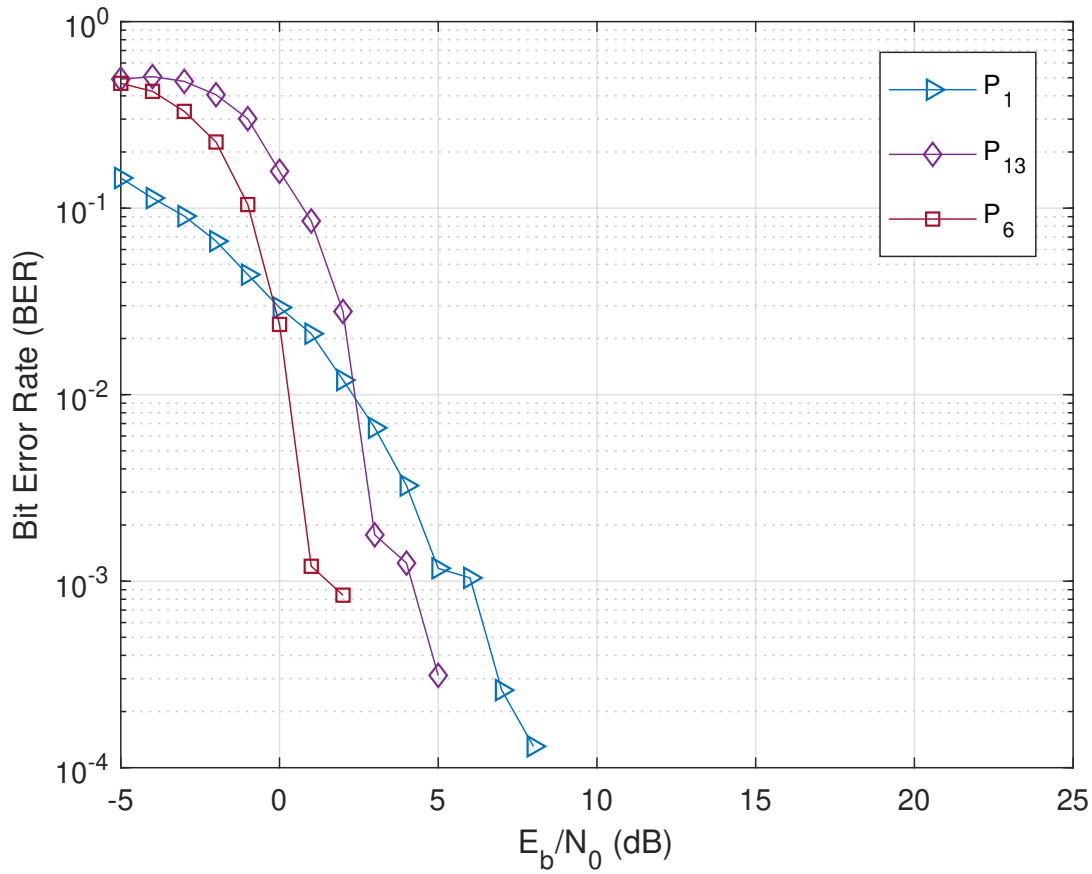


Figure 5.2: BER for various modes of operation in SUI-1

5.3.2 Data Attainment

Once the BER curves are obtained the data is procured by drawing a horizontal line for each QoS i.e. $\{E_1, E_2, E_3, E_4\}$ for all the BER curves and the intersection point gives a particular SNR value. This provides the minimum SNR guaranteeing the BER to be within maximum allowable value along with the achievable throughput for a specific MSC pair. The acquired data for AWGN, SUI-1 and SUI-4 cases are given in three dimensional tables as there are three parameters under consideration.

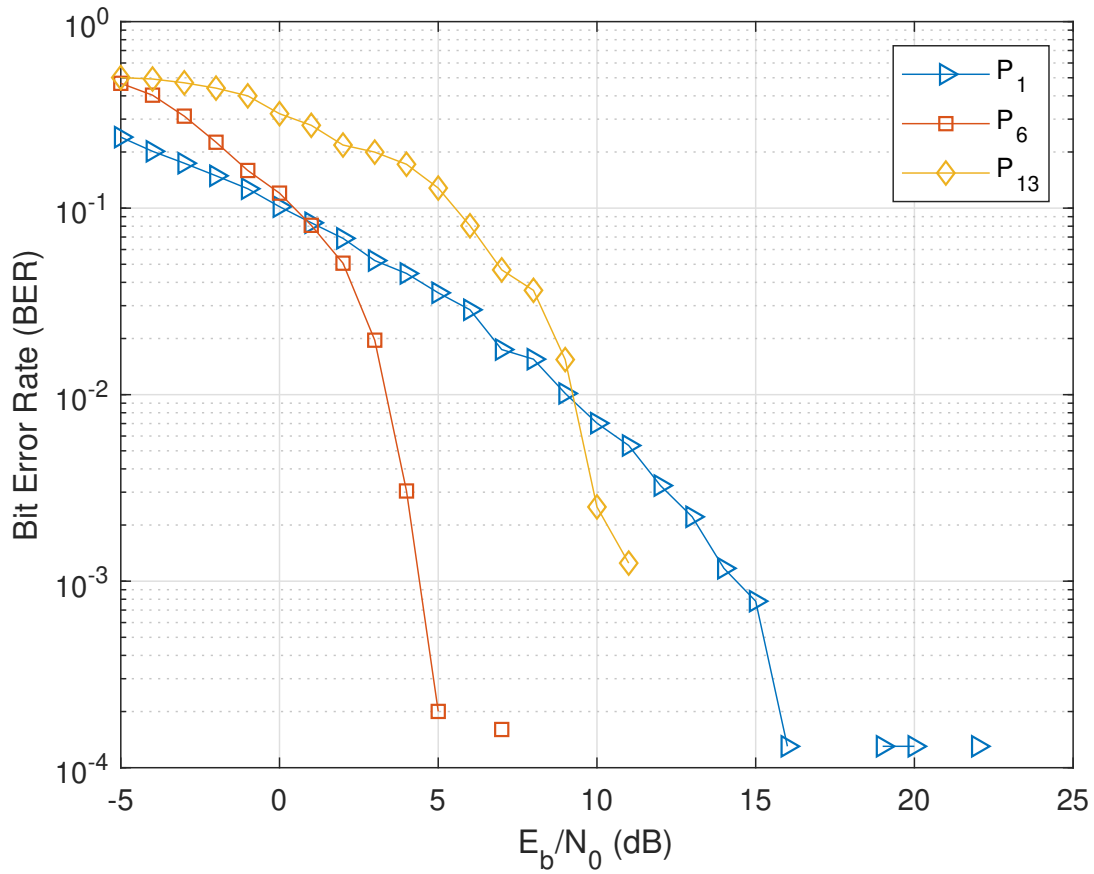


Figure 5.3: BER for various modes of operation in SUI-4

AWGN

For AWGN case the SNR data for $M = 2$ and $M = 4$ are given in the tables Table 5.5 and Table 5.6.

SUI-1

For SUI-1 case the SNR data for $M = 2$ and $M = 4$ are given in the tables Table 5.7 and Table 5.8.

Table 5.5: Data Acquisition for $M = 2$ in AWGN

N	BER	$r = 1$	$r = 2/3$	$r = 1/2$
128	E_1	-3.876	-1.716	-2.743
	E_2	1.183	-0.3463	-1.268
	E_3	3.607	-	-0.09797
	E_4	-	-	-
256	E_1	-3.897	-1.807	-2.745
	E_2	1.052	-0.5708	-1.245
	E_3	3.634	0.5355	-0.3204
	E_4	4.648	-	-
512	E_1	-3.924	-1.937	-2.597
	E_2	1.332	-0.5848	-1.325
	E_3	3.794	-	-0.3665
	E_4	5.351	-	-

SUI-4

For SUI-4 case the SNR data for $M = 2$ and $M = 4$ are given in the tables Table 5.9 and Table 5.10.

5.4 Proposed Condition Algorithm for Link Adaptation

After the data has been extracted for all the channels the last stage is the human intuition based selection of MSC pairs. The algorithm provides with the selection of most suitable MSC pair in order to provide with optimum transmission parameters according to the given

Table 5.6: Data Acquisition for $M = 4$ in AWGN

N	BER	$r = 1$	$r = 2/3$	$r = 1/2$
128	E_1	-3.816	-1.858	-2.576
	E_2	1.309	-0.5682	-1.12
	E_3	3.721	-	-0.1174
	E_4	5.412	-	-
256	E_1	-3.992	-1.883	-2.664
	E_2	1.336	-0.6017	-1.134
	E_3	3.659	0.2375	-0.1663
	E_4	5.354	-	-
512	E_1	-3.957	-1.852	-2.588
	E_2	1.196	-0.5561	-1.216
	E_3	3.779	0.2271	-0.354
	E_4	5.33	0.7478	-

conditions. It comprises of a collection of logic rules in the form of IF-THEN statements. The 'IF' part of the rule is called 'antecedent' and the 'THEN' part of the rule is called 'consequent'. The proposed algorithm takes three inputs i.e. required QoS from the user, user Data rate requirement and available channel SNR and gives one MSC pair among the 18 pairs as mentioned earlier in the Table 5.4. The adaptive algorithm can be represented by the following Fig. 5.4.

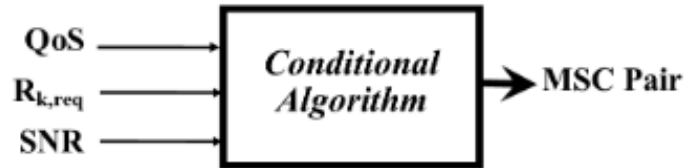


Figure 5.4: Conditional Rule based Cognition Engine

Table 5.7: Data Acquisition for $M = 2$ in SUI-1

N	BER	$r = 1$	$r = 2/3$	$r = 1/2$
128	E_1	-3.312	-1.198	-1.015
	E_2	2.426	0.355	0.3845
	E_3	6.034	1.00	-
	E_4	-	-	-
256	E_1	-3.403	-1.311	-0.4092
	E_2	2.115	0.3858	1.294
	E_3	4.457	-	-
	E_4	-	-	-
512	E_1	-3.764	-0.8224	-2.311
	E_2	1.521	1.005	-0.345
	E_3	4.003	1.792	0.9175
	E_4	-	-	-

The total number of rules based upon the acquired three dimensional data are $R_n = 64$. Let the inputs (QoS, $R_{k,req}$ and SNR) to the system be a_1^n , a_2^n , a_3^n respectively and the output MSC pair b^n be the n^{th} rule. Then the proposed conditional algorithm can be represented as,

$$(a_1^n, a_2^n, a_3^n; b^n) \quad n = 1, 2, 3, \dots, R_n$$

The selected pairs based upon above mentioned rule based are listed in the Table 5.11 for AWGN, Table 5.12 for SUI-1 and Table 5.13 for SUI-4. Conditional rules could be widely categorized in two different scenarios:

- Concurring Rules
- Conflicting Rules

Table 5.8: Data Acquisition for $M = 4$ in SUI-1

N	BER	$r = 1$	$r = 2/3$	$r = 1/2$
128	E_1	-2.906	-0.8757	-0.6172
	E_2	3.483	1.096	0.6868
	E_3	6.669	2.356	1.729
	E_4	-	-	-
256	E_1	-3.212	-0.9574	-0.3896
	E_2	2.312	0.8006	0.9616
	E_3	5.153	1.754	1.493
	E_4	-	-	-
512	E_1	-3.651	0.06995	-1.007
	E_2	1.733	1.461	1.345
	E_3	4.566	3.073	2.891
	E_4	7.312	-	-

5.4.1 Concurring Rules

The rules which have same antecedent as well as consequent are termed as Concurring Rules. The required QoS i.e. E , SNR i.e. S and data rate i.e. R agree with each other in this case and the resultant output is a single mode of operation. In the case if two or more consequent result in same throughput, the mode offering least complexity is chosen. In our case considering the parameters, the increase in the modulation order or the number of subcarriers, the complexity is enhanced [66]. The convolutional encoding has a negligible effect in case of code rate 2/3 due to enhanced trace-back length because of utilizing puncturing for Viterbi Decoder [36].

Table 5.9: Data Acquisition for $M = 2$ in SUI-4

N	BER	$r = 1$	$r = 2/3$	$r = 1/2$
128	E_1	0.1162	2.242	3.217
	E_2	9.307	6.654	6.366
	E_3	15.11	-	-
	E_4	-	-	-
256	E_1	0.7874	3.294	2.853
	E_2	6.099	5.103	4.833
	E_3	9.572	6.318	5.531
	E_4	-	-	-
512	E_1	-2.602	0.4634	-0.4786
	E_2	4.43	3.796	3.158
	E_3	8.723	-	4.384
	E_4	13.57	-	5.508

5.4.2 Conflicting Rules

If a rule has same antecedent but different consequent, it is termed as a Conflicting Rule. For this case the pair providing with better throughput would be selected. In case if for a specific quality there is no mode available at higher SNR, but there is a mode available at lower SNR, the mode present at lower SNR should be selected as it would of course run if the SNR is raised. If there is no mode available for a higher quality of service, then the best possible mode available at lower QoS must be selected.

As an example Fig.5.5 presents the case with $E_2, S_1, R_1, E_3, S_2, R_2$ in Fig.5.6 and Fig.5.7 presents the set with E_3, S_1, R_2 the data acquisition for SUI-4 model.

For the proof of concept, let's discuss a few selected modes of operation, according to the user requirements as well as the available channel conditions. Fig. 5.8 presents a

Table 5.10: Data Acquisition for $M = 4$ in SUI-4

N	BER	$r = 1$	$r = 2/3$	$r = 1/2$
128	E_1	0.8662	6.098	3.489
	E_2	11.81	9.329	7.982
	E_3	21.79	12.83	8.909
	E_4	-	-	-
256	E_1	0.1619	3.115	2.626
	E_2	7.704	6.122	5.229
	E_3	17.97	7.332	-
	E_4	-	-	-
512	E_1	-2.305	0.4095	-0.3931
	E_2	4.477	3.921	3.162
	E_3	9.037	5.09	4.525
	E_4	12.94	-	-

situation where the quality of service requirement is 10^{-2} , SNR availability lies between 4dB to 11dB, and the required data rates range is 6Mbps to 8Mbps. The selected mode from the algorithm is P_{13} that achieves the desired need within the available channel conditions at about 9.053dB. So the transmitting end parameters that mode P_{13} provides i.e. MSC (4,128,2/3) are considered to be optimum.

In the Fig. 5.9, the quality of service is now at 10^{-3} , SNR between 4dB to 11dB, and the required data rates range is 4Mbps to 6Mbps, that is given a mode of P_2 . The assigned parameters for this mode are MSC(2,256,1) that have achieved the desired characteristics at about 9.179dB.

And lastly, let's discuss a case where the available channel conditions are way better, lying within an SNR range of 18dB to 25dB, but the assigned mode is P_8 , that reaches the required throughput as well as quality of service at just 5.894dB. Even though

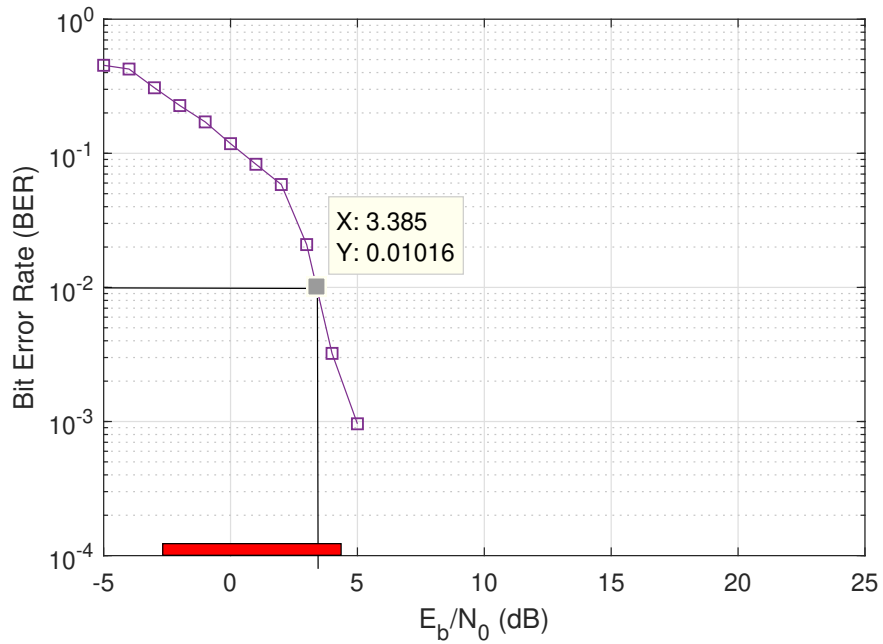


Figure 5.5: Data Acquisition for E_2, S_1, R_1

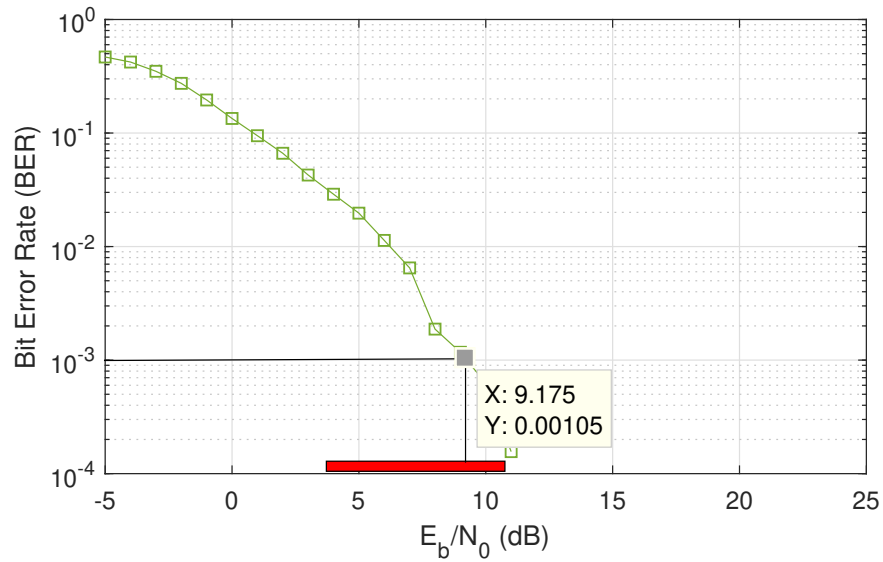


Figure 5.6: Data Acquisition for E_3, S_2, R_2

the channel conditions here are fair enough to allow higher data rates, we have limited the user to the required data rate of 2Mbps to 4Mbps, so as to avoid the complexity as well as for the transmitting end power conservation. The case is illustrated in Fig. 5.10.

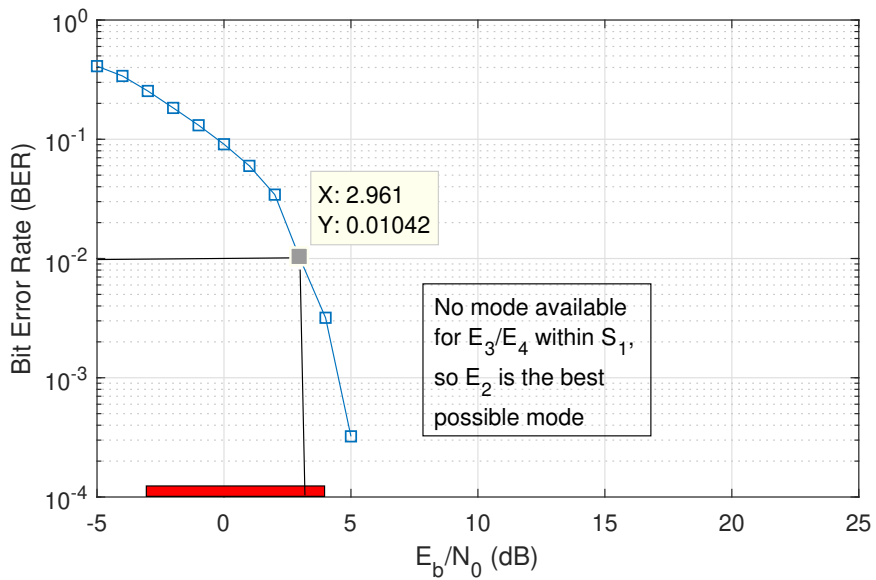


Figure 5.7: Data Acquisition for E_3 , S_1 , R_2

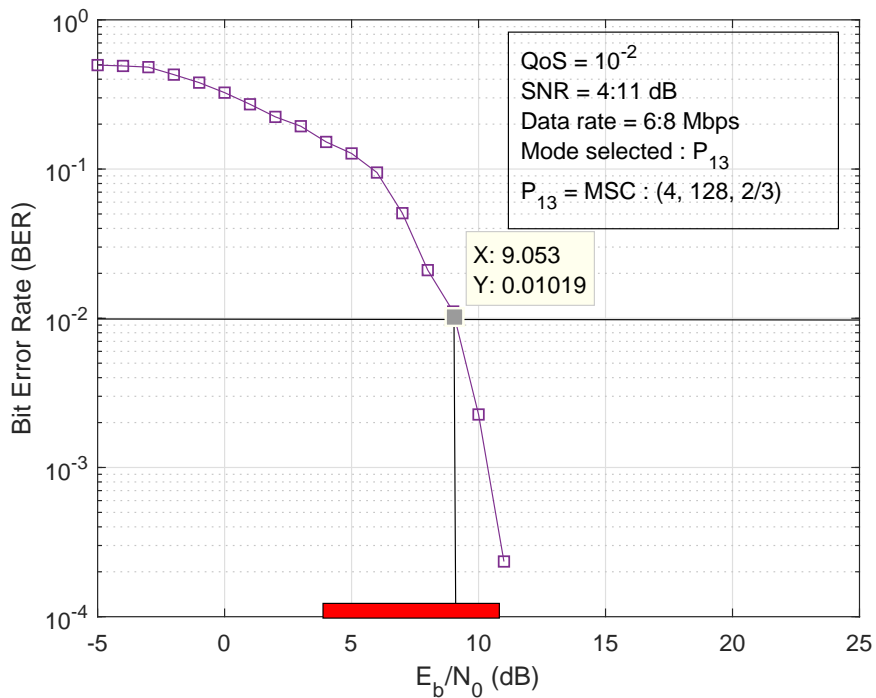


Figure 5.8: Mode selection for QoS of 10^{-2} , SNR from 4dB to 11dB, required data rates range 6Mbps to 8Mbps

Table 5.11: Conditional Rules for AWGN Channel

QoS	SNR	R_1	R_2	R_3	R_4
E_1	S_1	P_7	P_1	P_{10}	P_{10}
	S_2	P_4	P_{13}	P_{13}	P_{13}
	S_3	P_4	P_{13}	P_{13}	P_{13}
	S_4	P_4	P_{13}	P_{13}	P_{13}
E_2	S_1	P_7	P_1	P_{10}	P_{10}
	S_2	P_4	P_{16}	P_{13}	P_{13}
	S_3	P_{10}	P_1	P_{10}	P_{10}
	S_4	P_{10}	P_1	P_{10}	P_{10}
E_3	S_1	P_7	P_1	P_{10}	P_{10}
	S_2	P_5	P_{16}	P_{14}	P_{14}
	S_3	P_{10}	P_1	P_{10}	P_{10}
	S_4	P_{10}	P_1	P_{10}	P_{10}
E_4	S_1	P_7	P_1	P_{10}	P_{10}
	S_2	P_{15}	P_{15}	P_{15}	P_{15}
	S_3	P_{15}	P_{15}	P_{15}	P_{15}
	S_4	P_{15}	P_2	P_{10}	P_{10}

5.4.3 Conditional Algorithm Flowchart

The detailed flowchart for the proposed human intuition based conditional algorithm is shown in the Fig. 5.11. The algorithm starts by taking two inputs i.e. the available SNR and required QoS by the user. If there exist some modes of operation that lie within this E and S bracket, then the third input of required data rate is given. After the final input if a single mode is extracted from this bracket, it would be considered as the optimum mode of operation and such rules would be termed as concurring rules.

Table 5.12: Conditional Rules for SUI-1 Channel

QoS	SNR	R_1	R_2	R_3	R_4
E_1	S_1	P_9	P_1	P_{10}	P_{10}
	S_2	P_4	P_{16}	P_{13}	P_{13}
	S_3	P_4	P_{16}	P_{13}	P_{13}
	S_4	P_4	P_{16}	P_{13}	P_{13}
E_2	S_1	P_9	P_1	P_{10}	P_{10}
	S_2	P_4	P_{14}	P_{14}	P_{14}
	S_3	P_8	P_1	P_{13}	P_{10}
	S_4	P_8	P_1	P_{13}	P_{10}
E_3	S_1	P_9	P_1	P_{10}	P_{10}
	S_2	P_6	P_6	P_6	P_6
	S_3	P_{13}	P_{16}	P_{13}	P_{13}
	S_4	P_{10}	P_1	P_{10}	P_{10}
E_4	S_1	P_9	P_1	P_{10}	P_{10}
	S_2	P_6	P_6	P_6	P_6
	S_3	P_{13}	P_{16}	P_{13}	P_{13}
	S_4	P_{12}	P_{12}	P_{12}	P_{12}

On the other hand, the conflicting rules incorporate diverse consequent possibilities, such as if there are no modes within the bracket of E and S with the required QoS, the optimum mode would be considered the mode previously available providing the best available QoS. Similarly, if there is no mode meeting the required SNR, the mode available at the lower SNR would be considered. This because if a mode is running at a lower SNR, it would work for a higher vale of SNR as well.

After the third input of data rate, if a single mode is not obtained from the E , S and R bracket, there could be two cases. If the bracket is providing no mode that is

Table 5.13: Conditional Rules for SUI-4 Channel

QoS	SNR	R_1	R_2	R_3	R_4
E_1	S_1	P_7	P_1	P_{14}	P_{10}
	S_2	P_7	P_1	P_{13}	P_{10}
	S_3	P_7	P_1	P_{13}	P_{10}
	S_4	P_7	P_1	P_{13}	P_{10}
E_2	S_1	P_6	P_{18}	P_{15}	P_{15}
	S_2	P_7	P_1	P_{13}	P_{11}
	S_3	P_7	P_1	P_{13}	P_{10}
	S_4	P_7	P_1	P_{13}	P_{10}
E_3	S_1	P_6	P_{18}	P_{15}	P_{15}
	S_2	P_8	P_2	P_{14}	P_{12}
	S_3	P_8	P_1	P_{13}	P_{11}
	S_4	P_8	P_1	P_{13}	P_{10}
E_4	S_1	P_6	P_{18}	P_{15}	P_{15}
	S_2	P_9	P_{18}	P_{15}	P_{15}
	S_3	P_9	P_3	P_{15}	P_{12}
	S_4	P_9	P_3	P_{15}	P_{12}

fulfilling the required data rate, the mode that is granting maximum throughput should be considered optimum. Contrarily, if there are more than one mode within the bracket after the third input, the computational complexity difference is observed among all the multiple modes. If a significant complexity difference is present, the mode with the least complexity should be considered best. While on account of negligible computational complexity difference, the mode providing better throughput is extracted from the bracket.

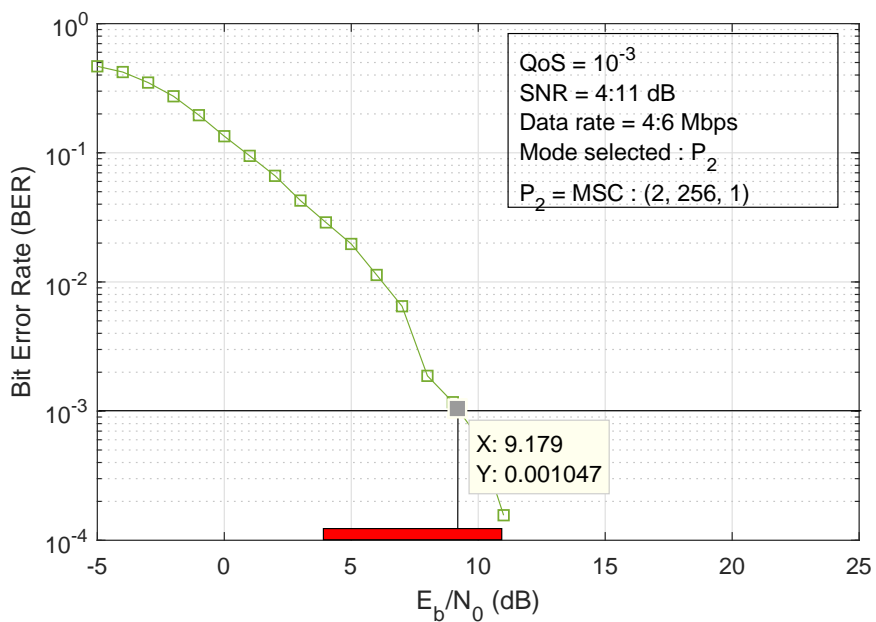


Figure 5.9: Mode selection for QoS of 10^{-3} , SNR from 4dB to 11dB, required data rates range 4Mbps to 6Mbps

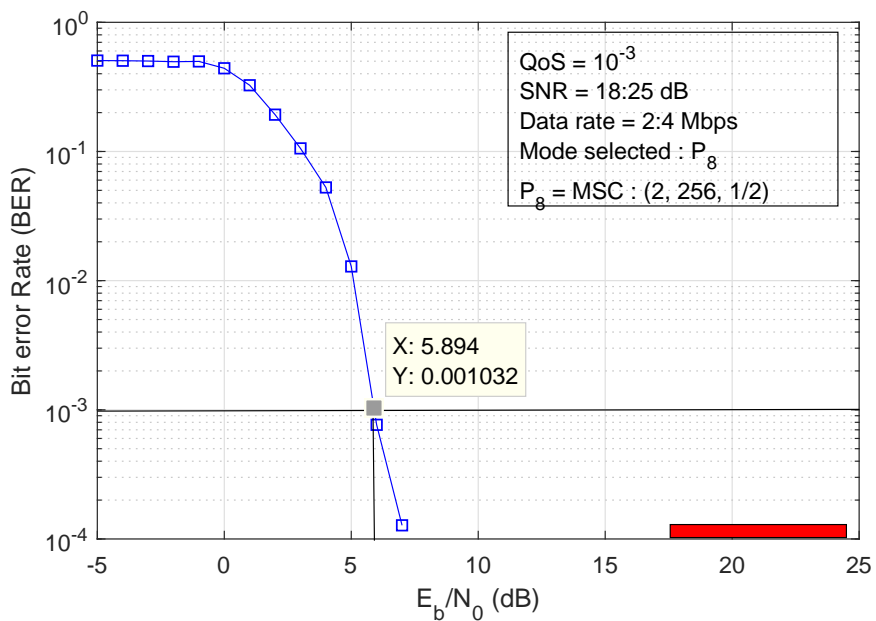


Figure 5.10: Mode selection for QoS of 10^{-3} , SNR from 18dB to 25dB, required data rates range 2Mbps to 4Mbps

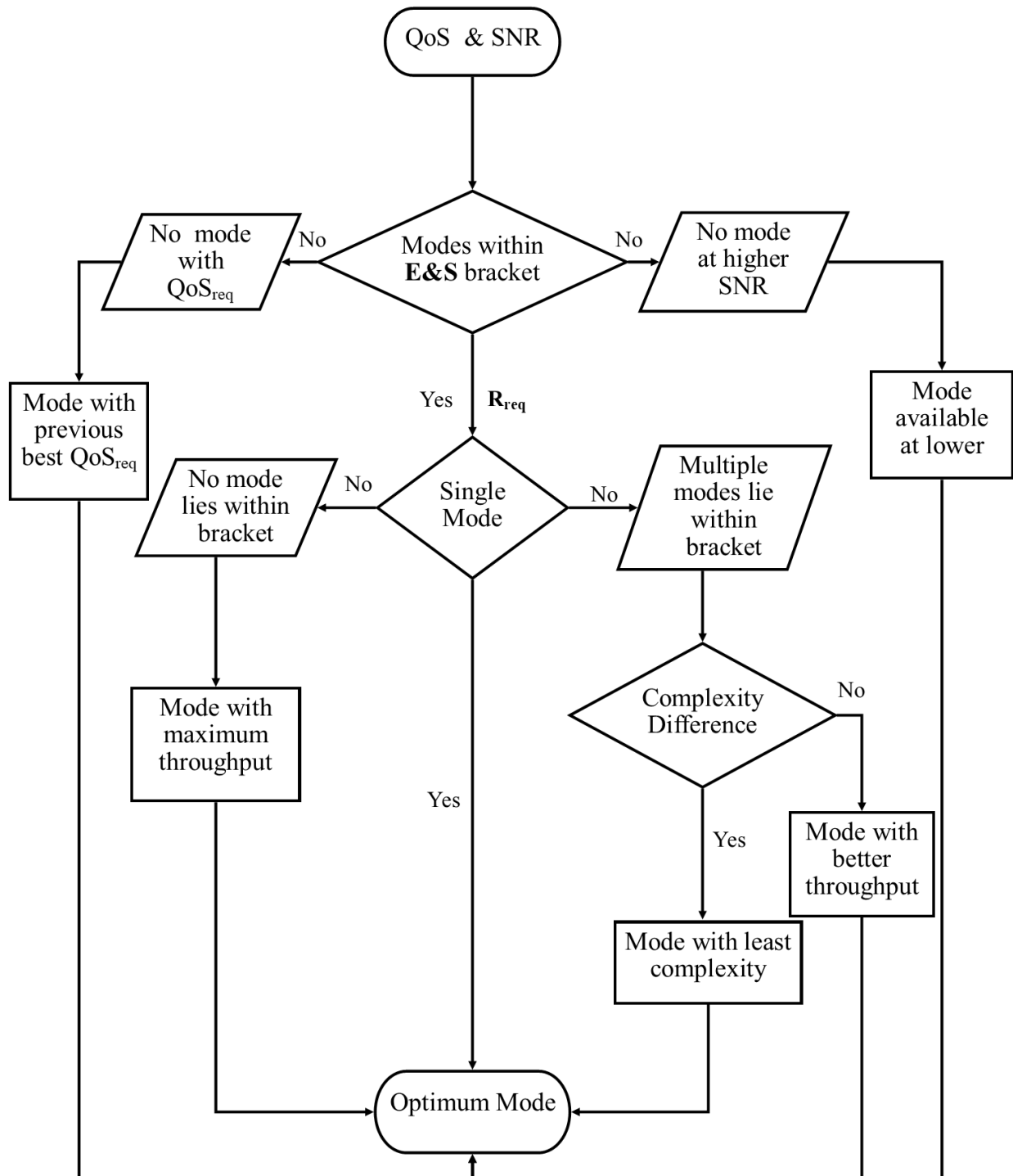


Figure 5.11: Conditional Algorithm Flowchart

Chapter 6

Conclusion and Future Work

6.1 Conclusion

The evolution of wireless communications standards and the rising number of users demand an efficient resource allocation of the available radio frequency spectrum for the SDR platform. The variable user requirements and fluctuating channel conditions need to be incorporated via link adaptation in order to provide well-organized utilization of RF bandwidth.

In this thesis, we have proposed an Adaptive Modulation and Coding based link adaptation algorithm, with the underlying scheme of Filterbank Multicarrier modulation. The whole thesis has been divided into three phases of research methodology. The first phase is the system model formulation where the FBMC system model is formulated incorporating convolutional encoding, Offset-QAM modulation and MMSE equalization. A comparative analysis between OFDM and FBMC based on the BER simulation results within both AWGN and multipath fading environment is done. The performance results indicate that OFDM reaches noise floor when used for SUI-4 channel having moderate-to-heavy tree density. Whereas FBMC/OQAM provides significantly better performance within fading environment.

The second phase of implementation involves performance and parametric analysis. The performance analysis is done in order to observe the performance improvement when complex QAM modulation is replaced with OQAM and with the inclusion of convolutional encoding rates within the FBMC system. The parametric analysis has been done

on the basis of four different parameters; modulation order, number of subcarrier, encoding rate and overlapping factor. The increment in subcarrier count and overlapping factor shows an improvement in BER curves whereas decrements in modulation order and code rate improves the performance as well.

The final and paramount phase of research methodology is the development of adaptive algorithm that has been done through three stages. Firstly, the problem formulation is done by throughput calculation and putting the constraints of required data rate, keeping the BER below the maximum allowed BER or QoS. The next step is data acquisition from the performance curves for all the selected QoS and modes of operation. Once the data has been acquired, the final step is the establishment of human intuition based Conditional Rules based algorithm built on concurring and conflicting rules. A total of 64 such rules have been formulated for AWGN as well as SUI-1 and SUI-4 channels. The proposed algorithm ensures the most feasible selection of transmission parameters according to the user requirements and channel conditions.

6.2 Future Recommendations

This thesis provides a dynamic selection of optimum parameters based upon conditional algorithm that is a crucial requirement for SDR waveform design. In order to get a more comprehensive analysis following future directions could be considered.

- Being a multicarrier scheme like OFDM, FBMC suffers from high Peak to Average Power Ratio (PAPR) [67–69]. As a result, High Power Amplifiers(HPA) goes into the non-linearity region distorting the signal and reducing the overall efficiency of the system, leading to the use of high dynamic range of power amplifiers thus increasing the cost and power utilized [70]. Incorporating PAPR reduction techniques within the simulation model of FBMC/OQAM could prove economical in regards with cost of power amplifiers.

- To achieve packet re-transmission overhead and achieve even better throughput analysis Fuzzy Inference based Link Adaptation algorithm could prove to be further advantageous.
- In order to include versatility within the proposed algorithms, the adaptation should be investigated and enhanced by utilizing multiple varying RF bandwidths.
- Finally in order to get the proof of concept of the proposed algorithm and to demonstrate the implementation affinity of the proposed technology, the algorithms should be implemented using FPGA and DSP on real time SDR platform.

References

- [1] S. Kundrapu, S. I. Dutt, N. K. Koilada, and A. C. Raavi, “Characteristic Analysis of OFDM, FBMC and UFMC Modulation Schemes for Next Generation Wireless Communication Network Systems,” in *2019 3rd International Conference on Electronics, Communication and Aerospace Technology (ICECA)*. IEEE, 2019, pp. 715–721.
- [2] B. Farhang-Boroujeny and R. Kempter, “Multicarrier communication techniques for spectrum sensing and communication in cognitive radios,” *IEEE Communications Magazine*, vol. 46, no. 4, pp. 80–85, 2008.
- [3] A. Gupta and R. K. Jha, “A survey of 5G network: Architecture and emerging technologies,” *IEEE access*, vol. 3, pp. 1206–1232, 2015.
- [4] I. B. F. de Almeida, L. L. Mendes, J. J. Rodrigues, and M. A. da Cruz, “5G Waveforms for IoT Applications,” *IEEE Communications Surveys & Tutorials*, vol. 21, no. 3, pp. 2554–2567, 2019.
- [5] R. N. Mitra and D. P. Agrawal, “5G mobile technology: A survey,” *ICT Express*, vol. 1, no. 3, pp. 132–137, 2015.

- [6] M. Bellanger, D. Le Ruyet, D. Roviras, M. Terré, J. Nossek, L. Baltar, Q. Bai, D. Waldhauser, M. Renfors, T. Ihalainen *et al.*, “FBMC physical layer: a primer,” *Phydyas*, vol. 25, no. 4, pp. 7–10, 2010.
- [7] J. Rohde and T. S. Toftegaard, “Adapting cognitive radio technology for low-power wireless personal area network devices,” *Wireless Personal Communications*, vol. 58, no. 1, pp. 111–123, 2011.
- [8] M. S. John and J. Soumya, “Achieving Cognitive Radio for Improved Spectrum Utilization: An Implementation,” 2019.
- [9] F. K. Jondral, “Software-defined radio—basics and evolution to cognitive radio,” *EURASIP journal on wireless communications and networking*, vol. 2005, no. 3, p. 652784, 2005.
- [10] R. Krishnan, R. G. Babu, S. Kaviya, N. P. Kumar, C. Rahul, and S. S. Raman, “Software defined radio (SDR) foundations, technology tradeoffs: A survey,” in *2017 IEEE International Conference on Power, Control, Signals and Instrumentation Engineering (ICPCSI)*. IEEE, 2017, pp. 2677–2682.
- [11] C. O. F. Regulations, “Title 21,” *Chapter I (revised)*, 2000.
- [12] J. Mitola, “Softwareradios: Survey, Critical Evaluation and Future Directions, proc. National Telesystems Conference,” 1992.

- [13] D. Lau, J. Blackburn, and J. A. Seely, “The use of hardware acceleration in SDR waveforms,” in *Proc. 2006 Software Defined Radio Technical Conference (SDR’05)*, 2005, pp. 13–17.
- [14] X. Wei, H. Liu, Z. Geng, K. Zheng, R. Xu, Y. Liu, and P. Chen, “Software defined radio implementation of a non-orthogonal multiple access system towards 5G,” *IEEE Access*, vol. 4, pp. 9604–9613, 2016.
- [15] N. Tandon, B. Suman, N. Agarwal, and V. Bhatia, “Design and testability aspects of mobile adhoc networking waveform physical layer for software defined radio,” in *2017 International Conference on Computing, Communication and Automation (ICCCA)*. IEEE, 2017, pp. 453–457.
- [16] G. Ray, “Boeing Technical Journal On-Demand Waveform Design for Software Defined Radio Applications,” 2016.
- [17] K. K. Singh *et al.*, “A Survey Paper on Multicarrier Modulation Techniques,” in *2018 5th IEEE Uttar Pradesh Section International Conference on Electrical, Electronics and Computer Engineering (UPCON)*. IEEE, 2018, pp. 1–6.
- [18] R. N. Mitra and D. P. Agrawal, “5G mobile technology: A survey,” *ICT Express*, vol. 1, no. 3, pp. 132–137, 2015.

- [19] D. Bepari and D. Mitra, "Improved power loading scheme for orthogonal frequency division multiplexing based cognitive radio," *IET Communications*, vol. 9, no. 16, pp. 2033–2040, 2015.
- [20] J. Du and S. Signell, "Comparison of CP-OFDM and OFDM/OQAM in doubly dispersive channels," in *Future Generation Communication and Networking (FGCN 2007)*, vol. 2. IEEE, 2007, pp. 207–211.
- [21] R. Zakaria, "Transmitter and receiver design for inherent interference cancellation in MIMO filter-bank based multicarrier systems," Ph.D. dissertation, 2012.
- [22] A. Zafar, "Filter bank based multicarrier systems for future wireless networks." Ph.D. dissertation, University of Surrey, 2018.
- [23] B. D. Tensubam, N. L. Chanu, and S. Singh, "Comparative analysis of FBMC and OFDM multicarrier techniques for wireless communication networks," *International Journal of Computer Applications*, vol. 100, no. 19, 2014.
- [24] A. F. Isnawati, V. O. Citra, and J. Hendry, "Performance Analysis of Audio Data Transmission on FBMC-Offset QAM System," in *2019 IEEE International Conference on Industry 4.0, Artificial Intelligence, and Communications Technology (IAICT)*. IEEE, 2019, pp. 81–86.

- [25] A. I. Pérez-Neira, M. Caus, R. Zakaria, D. Le Ruyet, E. Kofidis, M. Haardt, X. Mestre, and Y. Cheng, “MIMO signal processing in offset-QAM based filter bank multicarrier systems,” *IEEE Transactions on Signal Processing*, vol. 64, no. 21, pp. 5733–5762, 2016.
- [26] J. Wen, J. Hua, W. Lu, Y. Zhang, and D. Wang, “Design of waveform shaping filter in the UFMC system,” *IEEE Access*, vol. 6, pp. 32 300–32 309, 2018.
- [27] A. Mohammadian, A. Mohammadi, A. Abdipour, and M. Baghani, “Spectral analysis of GFDM modulated signal under nonlinear behavior of power amplifier,” *arXiv preprint arXiv:1803.02026*, 2018.
- [28] S. Kaur, L. Kansal, G. S. Gaba, and N. Safarov, “Survey of Filter Bank Multicarrier (FBMC) as an efficient waveform for 5G,” *International Journal of Pure and Applied Mathematics*, vol. 118, no. 7, pp. 45–49, 2018.
- [29] S. Ramakrishna, S. B. Shirol, and P. Kumar, “A Comparative Evaluation of FBMC with OFDM over a Time-and Frequency-Selective Channel,” in *2018 International Conference on Electrical, Electronics, Communication, Computer, and Optimization Techniques (ICEECCOT)*. IEEE, 2018, pp. 800–803.
- [30] A. Ibrahim and M. Abdullah, “The potential of FBMC over OFDM for the future 5G mobile communication technology,” in *AIP Conference Proceedings*, vol. 1883, no. 1.

AIP Publishing LLC, 2017, p. 020001.

- [31] K. Hari, D. Baum, A. Rustako, R. Roman, and D. Trinkwon, “Channel models for fixed wireless applications,” *IEEE 802.16 Broadband wireless access working group*, 2003.
- [32] R. Jain, “Channel models: A tutorial,” in *WiMAX forum AATG*, vol. 10, 2007.
- [33] R. Kadel, N. Islam, K. Ahmed, and S. J. Halder, “Opportunities and Challenges for Error Correction Scheme for Wireless Body Area Network—A Survey,” *Journal of Sensor and Actuator Networks*, vol. 8, no. 1, p. 1, 2019.
- [34] R. A. Shams, M. H. Kabir, and S. E. Ullah, “Effect of Interleaved FEC Code on Wavelet based MC-CDMA System with Alamouti STBC in Different Modulation Schemes,” *arXiv preprint arXiv:1207.3884*, 2012.
- [35] S. Garg, A. K. Sharma, and A. Tyagi, “PERFORMANCE ANALYSIS OF 1/2 CODE RATE CONVOLUTION ENCODED DWT-OFDM SYSTEM WITH DIFFERENT MODULATION SCHEMES,” *Intl. J. Innovative Res. Sci. Eng.*, vol. 3, pp. 109–119, 2017.
- [36] F. Sandoval, G. Poitau, and F. Gagnon, “Optimizing forward error correction codes for COFDM with reduced PAPR,” *IEEE Transactions on Communications*, vol. 67, no. 7, pp. 4605–4619, 2019.

- [37] P. Elias, “Coding for noisy channels,” *IRE Conv. Rec.*, vol. 3, pp. 37–46, 1955.
- [38] F. Jelinek, “An upper bound on moments of sequential decoding effort,” *IEEE Transactions on Information Theory*, vol. 15, no. 1, pp. 140–149, 1969.
- [39] D. Achlioptas, H. Hassani, W. Liu, and R. Urbanke, “Time-invariant LDPC convolutional codes,” in *2017 IEEE International Symposium on Information Theory (ISIT)*. IEEE, 2017, pp. 366–370.
- [40] V. H. S. Le, C. A. Nour, E. Boutillon, and C. Douillard, “Dual Trellis Construction for High-Rate Punctured Convolutional Codes,” in *2019 IEEE 30th International Symposium on Personal, Indoor and Mobile Radio Communications (PIMRC Workshops)*, pages=1–7, year=2019, organization=IEEE.
- [41] J. Lieb, R. Pinto, and J. Rosenthal, “Convolutional Codes,” *arXiv preprint arXiv:2001.08281*, 2020.
- [42] J. Omura, “On the Viterbi decoding algorithm,” *IEEE Transactions on Information Theory*, vol. 15, no. 1, pp. 177–179, 1969.
- [43] H. Yamamoto and K. Itoh, “Viterbi decoding algorithm for convolutional codes with repeat request,” *IEEE Transactions on Information Theory*, vol. 26, no. 5, pp. 540–547, 1980.

- [44] S. Dhaliwal, N. Singh, and G. Kaur, "Performance analysis of convolutional code over different code rates and constraint length in wireless communication," in *2017 International Conference on I-SMAC (IoT in Social, Mobile, Analytics and Cloud)(I-SMAC)*. IEEE, 2017, pp. 464–468.
- [45] D. Haccoun and G. Begin, "High-rate punctured convolutional codes for Viterbi and sequential decoding," in *ITCom*, vol. 37, 1989, pp. 1113–1125.
- [46] C. L. Taylor, *Punctured convolutional coding scheme for multi-carrier multi-antenna wireless systems*. Electronics Research Laboratory, College of Engineering, University of . . . , 2001.
- [47] G. Miao, N. Himayat, and G. Y. Li, "Energy-efficient link adaptation in frequency-selective channels," *IEEE Transactions on communications*, vol. 58, no. 2, pp. 545–554, 2010.
- [48] W. N. W. Muhamad, S. S. Sarnin, A. Idris, and A. Syahira, "Link Adaptation Algorithm for IEEE 802.11 Wireless Local Area Networks in Fading Channel," *Indonesian Journal of Electrical Engineering and Computer Science*, vol. 12, no. 2, pp. 677–684, 2018.
- [49] M. Riback, S. Grant, G. Jongren, T. Tynderfeldt, D. Cairns, and T. Fulghum, "MIMO-HSPA testbed performance measurements," in *2007 IEEE 18th International Sympo-*

- sium on Personal, Indoor and Mobile Radio Communications.* IEEE, 2007, pp. 1–5.
- [50] J. Saha, S. S. Das, and S. Mukherjee, “Link Adaptation Using Dynamically Allocated Thresholds and Power Control,” *Wireless Personal Communications*, vol. 103, no. 3, pp. 2259–2283, 2018.
- [51] C. So-In, R. Jain, and A.-K. Tamimi, “Scheduling in IEEE 802.16 e mobile WiMAX networks: key issues and a survey,” *IEEE Journal on selected areas in communications*, vol. 27, no. 2, pp. 156–171, 2009.
- [52] M. A. Alavi, W. Fernando, P. Permuna, K. Jayathilake, S. Mathurusha, N. Vithanage, and D. Dhammearatchi, “Enhanced QoS support in OFDMA-Based WiMAX Systems,” *Compusoft*, vol. 5, no. 4, p. 2090, 2016.
- [53] B. S. K. Reddy and B. Lakshmi, “Adaptive modulation and coding for mobile-WiMAX using SDR in GNU radio,” in *2014 International Conference on Circuits, Systems, Communication and Information Technology Applications (CSCITA)*. IEEE, 2014, pp. 173–178.
- [54] “Adaptive Modulation and Coding with Channel State information in OFDM for WiMAX, author=Reddy, B Siva Kumar and Lakshmi, B, journal=IJ Image, Graphics and Signal Processing, volume=1, pages=61–69, year=2015.”

- [55] L. Wan, H. Zhou, X. Xu, Y. Huang, S. Zhou, Z. Shi, and J.-H. Cui, "Adaptive modulation and coding for underwater acoustic OFDM," *IEEE Journal of Oceanic Engineering*, vol. 40, no. 2, pp. 327–336, 2014.
- [56] M. Dottling, B. Raaf, and J. Michel, "Efficient channel quality feedback schemes for adaptive modulation and coding of packet data," in *IEEE 60th Vehicular Technology Conference, 2004. VTC2004-Fall. 2004*, vol. 2. IEEE, 2004, pp. 1243–1247.
- [57] S.-Y. Jeon and D.-H. Cho, "Channel adaptive CQI reporting schemes for HSDPA systems," *IEEE Communications Letters*, vol. 10, no. 6, pp. 459–461, 2006.
- [58] M. Q. Abdulhasan, M. I. Salman, C. K. Ng, N. K. Noordin, S. J. Hashim, and F. B. Hashim, "A threshold feedback compression scheme of channel quality indicator (CQI) in LTE systems," in *2013 IEEE Student Conference on Research and Development*. IEEE, 2013, pp. 181–186.
- [59] M. S. Khairy, A. Khajeh, A. M. Eltawil, and F. J. Kurdahi, "Joint power management and adaptive modulation and coding for wireless communications systems with unreliable buffering memories," *IEEE Transactions on Circuits and Systems I: Regular Papers*, vol. 61, no. 8, pp. 2456–2465, 2014.
- [60] M. Zeeshan and S. A. Khan, "A novel fuzzy inference-based technique for dynamic link adaptation in SDR wideband waveform," *IEEE Transactions on Communications*,

vol. 64, no. 6, pp. 2602–2609, 2016.

- [61] R. S. Janaki and V. Nagarajan, “FUZZY LOGIC BASED ADAPTIVE MODULATION SYSTEM FOR ENERGY EFFICIENT WIRELESS SENSOR NETWORK,” 2018.
- [62] Z. Yang, L. Cai, A. Gulliver, L. He, and J. Pan, “Beyond Powers of Two: Hexagonal Modulation and Non-Binary Coding for Wireless Communication Systems,” *arXiv preprint arXiv:1712.07630*, 2017.
- [63] H. C. Mora, N. O. Garzón, and C. de Almeida, “On the cellular spectral efficiency of MC-CDMA systems with MMSE multiuser detector employing fractional and soft frequency reuse,” *AEU-International Journal of Electronics and Communications*, vol. 84, pp. 34–45, 2018.
- [64] K. Shahzad, S. Gulzar, M. Zeeshan, and S. A. Khan, “A novel hybrid narrow-band/wideband networking waveform physical layer for multiuser multiband transmission and reception in software defined radio,” *Physical Communication*, vol. 36, p. 100790, 2019.
- [65] A. J. Tiwana and M. Zeeshan, “Parametric analysis of fbmc/oqam under sui fading channel models,” in *2020 22nd International Conference on Advanced Communication Technology (ICACT)*. IEEE, 2020, pp. 207–211.

- [66] B. Ahmed and M. Zeeshan, "Effect of Carrier Frequency Offset on the Performance of FBMC and GFDM under Multipath Fading Channels," in *2018 21st International Symposium on Wireless Personal Multimedia Communications (WPMC)*. IEEE, 2018, pp. 240–245.
- [67] S. K. C. Bulusu, H. Shaiek, D. Roviras, and R. Zayani, "Reduction of PAPR for FBMC-OQAM systems using dispersive SLM technique," in *2014 11th International Symposium on Wireless Communications Systems (ISWCS)*. IEEE, 2014, pp. 568–572.
- [68] I. A. Shaheen, A. Zekry, F. Newagy, and R. Ibrahim, "Performance evaluation of PAPR reduction in FBMC system using nonlinear companding transform," *ICT Express*, vol. 5, no. 1, pp. 41–46, 2019.
- [69] —, "PAPR reduction of FBMC/OQAM systems based on combination of DST precoding and A-law nonlinear companding technique," in *2017 International Conference on Promising Electronic Technologies (ICPET)*. IEEE, 2017, pp. 38–42.
- [70] P. Yang and A. Hu, "Two-piecewise companding transform for PAPR reduction of OFDM signals," in *2011 7th International Wireless Communications and Mobile Computing Conference*. IEEE, 2011, pp. 619–623.